

Dinoop Lal S. “Photodegradation of polystyrene by nano titanium dioxide and photosensitizers.” Thesis. Research & Postgraduate Department of Chemistry, St. Thomas’ College (Autonomous), Thrissur, University of Calicut, 2020.

Chapter 6

UV Degradation of Polystyrene using Organic Photosensitizers Coupled and Uncoupled with Nano TiO₂

Abstract

Photodegradation of PS was studied in the presence of a few benzophenone derivatives and triphenylmethane dyes as photosensitizers. The benzophenone derivatives acted as effective photosensitizers for the UV degradation of PS. Triphenylmethane dyes on the other hand were not appreciable photosensitizers for the photodegradation of PS. Photocatalytic activity of TiO₂ enhanced considerably in the presence of benzophenone derivatives and triphenylmethane dyes. Photocatalytic activity of benzophenones, under of UV light could be explained on the basis of diradicaloid formation. The difficulty in diradicaloid formation of 2-hydroxy-4-methoxybenzophenone (2HO4MOBP) due to photoenolization made it a weaker photosensitizer, compared to the other benzophenone derivatives under study. It was evident from the FTIR spectra that formation of alkenic double bonds dominated over other oxygen containing functional groups when PS-benzophenone based photosensitizer composites were subjected to UV irradiation.

6.1. Introduction

The effect of various substituted benzophenone and triphenylmethane dyes which acts as photosensitizers for the photodegradation of polystyrene (PS) is studied in this chapter. The photocatalytic efficiency of nano TiO₂ in the presence of these photosensitizers is also studied. Benzophenone (BP) is a renowned photosensitizer used in various photochemical reactions including photodegradation of polymers^{1,2}. The photodegradation of PS by BP has been extensively studied³⁻⁷. BP absorbs UV radiation leading to homolytic cleavage of the π bond belonging to its $>C=O$ group producing radicals. The photochemistry of BP is based on the reaction of these radicals with another species before recombination. The two phenyl rings directly connected to the carbonyl carbon are in conjugation with it. This ensures the stability of the radicals formed, minimizing the chance of recombination up to an extent. The radicals can be transferred to the neighbouring molecules initiating different types of photochemical reactions according to the nature of molecules. These reactions are named as *triplet-triplet energy transfer (T-TET)*, *type I electron transfer*, *type I H-abstraction* and *type II singlet oxygen* process⁸. In T-TET process, the spin and the energy are transferred between excited triplet state of benzophenone (³BP*) and the neighbouring molecule as elucidated in figure 6.1.

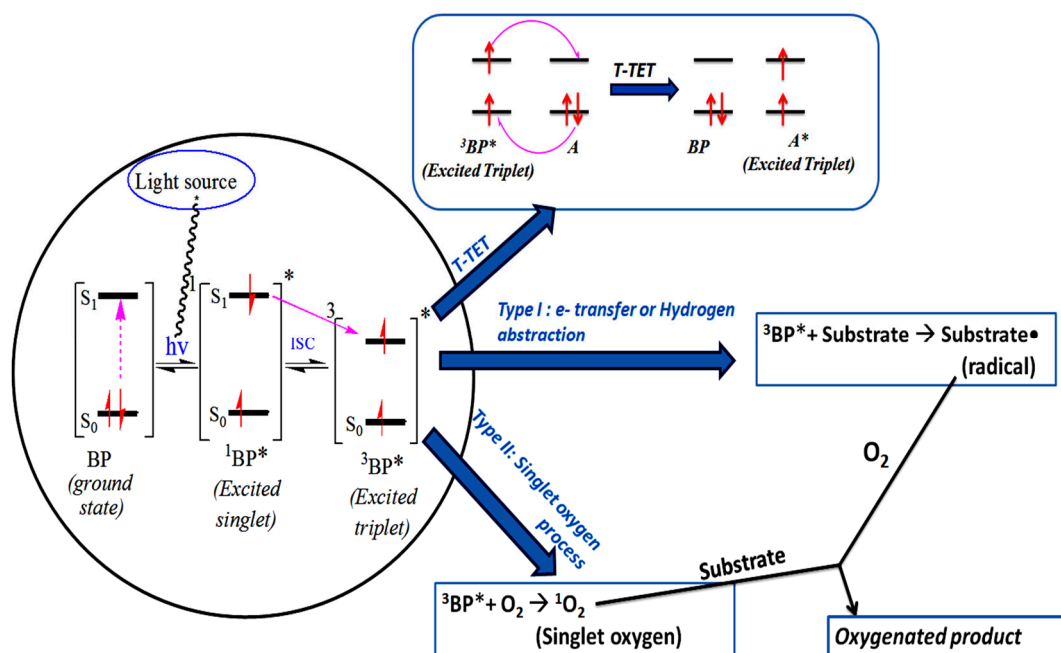


Figure 6.1. Photoreactions of benzophenone

T-TET in BP-naphthalene^{9,10} and BP-fluorine-naphthalene¹¹ systems have been reported. *Type I* processes take place when $^3\text{BP}^*$ reacts with neighbouring substrate or solvent. Electron transfer or hydrogen abstraction takes place during *type I* process. The result of this reaction is formation of radicals in the solvent or substrate molecules triggering radical initiated photochemical reactions in most cases. *Type II singlet oxygen* process take place when $^3\text{BP}^*$ reacts with oxygen. Singlet oxygen is produced as a consequence of these reactions by energy transfer which are reactive and can interact with another substrate to initiate photochemical reactions¹².

The stability of the radicals in $^3\text{BP}^*$ is the key factor that determines all types of energy transfer or processes discussed above. The stability of the radicals in $^3\text{BP}^*$ can be increased by increasing the aromaticity of the phenyl rings in the system. Substitution of electron donating groups on the phenyl ring can increase their aromaticity. Substituted benzophenones containing electron releasing as well as withdrawing groups have been chosen in this study and their photocatalytic efficiency have been compared with that of unsubstituted benzophenone for the photodegradation of PS under UV radiation.

The absorption of benzophenone is limited to the UV region of the spectrum. The use of selective organic dyes in the place of BP comes into picture in this point of view. Organic dyes can absorb in the UV as well as visible region. Organic dyes have been extensively used in various applications especially in the fields of dye sensitized solar cells (DSSC)^{13,14}, organic light emitting diodes (OLED)^{15,16}, liquid crystals (LC)^{17,18}, sensors for photoconductivity¹⁹ and so on. Dye photosensitized photodegradation of polymers has also been studied^{20,21}. Triphenylmethane dyes (methyl blue and malachite green) have been adopted as photosensitizer for PS photodegradation in this study. Triphenylmethane dyes are cheap with an attractive property of their brilliant colours²². Dyes also exhibit amazing properties in association with other substances. For example, proteins bonded to triphenylmethane dyes exhibit enhanced quantum yield, photo reactivity, intersystem crossing and fluorescence. The interaction of these dyes with proteins through type I electron or hydrogen transfer process as explained above resulted in these enhanced properties²³. Polymers incorporated with triphenylmethane dyes are widely used in various fields

including medicines, waste water treatments, gas separation, painting industry, dyeing process etc²⁴.

TiO₂ coupled with BP photosensitizers as well as with triphenylmethane dyes promises an effective photocatalyst with enhanced properties. TiO₂-BP blend has proven to be an efficient photocatalyst for the photo-oxidative degradation of polyethylene. The interaction of BP with the hydroxy (OH•) and hydroperoxy (OOH•) radicals (which are produced by interaction of the electrons and holes produced in TiO₂ with water and oxygen) leading to further radical formation on exposure to sunlight have been discussed here. The radical products react with the polyethylene chain resulting to its photodegradation²⁵. When triphenylmethane dyes are coupled with TiO₂, the mechanism is rather different. The dye absorbs light radiation in the visible and UV region leading to charge separation at the interface of TiO₂ and dye. The process termed as photo induced electron injection leads to the charge transport from excited dyes into the conduction band of TiO₂²⁶.

Section:I

UV degradation of polystyrene using benzophenone derivatives and organic dyes as photosensitizers

Photodegradation of PS using benzophenone derivatives and triphenylmethane dyes has been discussed in this section. The benzophenone derivatives are hereafter termed as '*benzophenone based photosensitizers*' and the triphenyl methyl dyes are termed as '*dye photosensitizers*'. The benzophenone based photosensitizers included in this study are benzophenone (BP), 2-hydroxy-4-methoxybenzophenone (2HO4MOBP), 4-methoxybenzophenone (4MOBP), 2-chlorobenzophenone (2ClBP) and 4-nitrobenzophenone (4NBP). The dye photosensitizers included in this study are malachite green (MG) and methyl blue (MB).

Structure and properties of the benzophenone based photosensitizers and dye photosensitizers included in this work are as tabulated in tables 6.1.1 and 6.1.2.

Table 6.1.1. List of benzophenone based photosensitizers

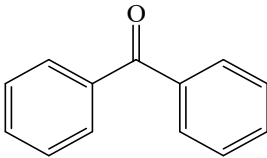
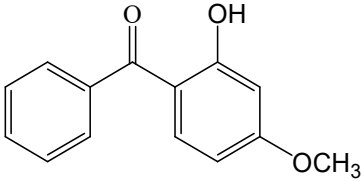
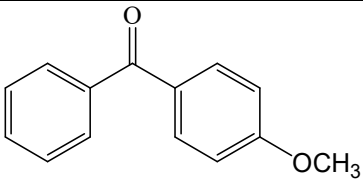
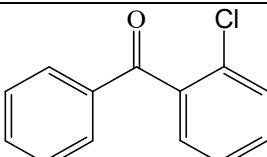
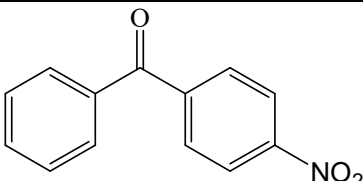
Benzophenone based photosensitizers				
Structure	Name	Abbreviation	Boiling point (°C)	Melting point (°C)
	Benzophenone	BP	305.4	48.5
	2-hydroxy-4-methoxybenzophenone	2HO4MOBP	150-160	62-64
	4-methoxybenzophenone	4MOBP	354-356	60-63
	2-chlorobenzophenone	2ClBP	330	44-47
	4-nitrobenzophenone	4NBP	390±25	136-138

Table 6.1.2. List of dye photosensitizers

Dye photosensitizers				
Structure	Name	Abbreviation	Boiling point (°C)	Melting point (°C)
	Malachite green	MG	520.91	158-160
	Methyl blue	MB	-	-

The preparation of PS-dye and PS-benzophenone based photosensitizer composites were as explained in chapter 2. The required weight percentage of the photosensitizers was incorporated into the PS. Specimens for electrical and mechanical measurements were also prepared.

6.2. Results and Discussion

6.2.1. Gel permeation chromatography (GPC)

The \bar{M}_w and \bar{M}_n of PS loaded with benzophenone based photosensitizers (Figure 6.2.1) as well as dye photosensitizers (Figure 6.2.2) decreased with respect to UV irradiation time. Comparative decrease in the average molecular weights upon UV irradiation showed only slight variation among the composites. The decrease in \bar{M}_w

and \bar{M}_n among PS-benzophenone based photosensitizer composites was found to be maximum in PS-4MOBP and minimum in PS-2HO4MOBP compared to their other counterparts under study (Figure 6.2.1). Among the PS-dye composites, the extent of decrease in the average molecular weights of PS-MG and PS-MB were almost similar upon UV irradiation. PS-MB however exhibited slightly enhanced reduction in the average molecular weights compared to that of PS-MG composite (Figure 6.2.2).

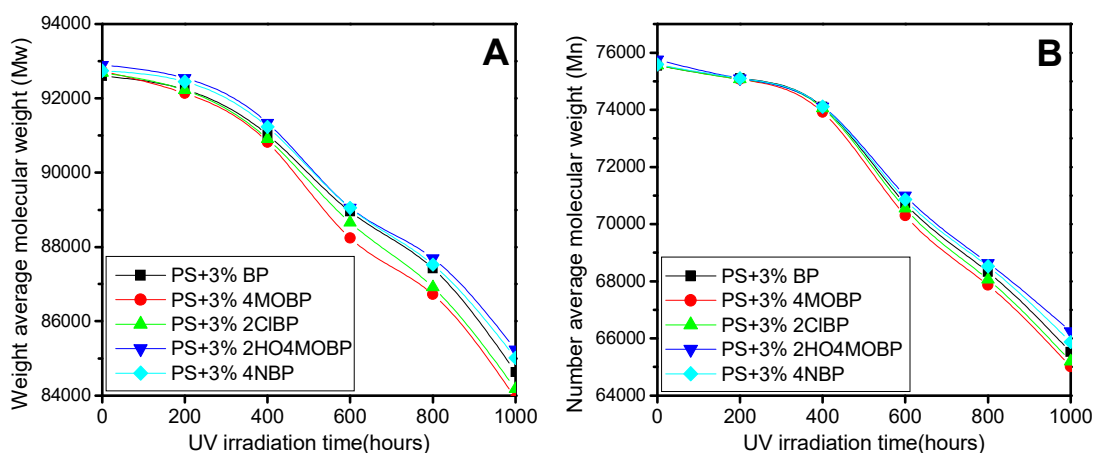


Figure 6.2.1. *A) Weight average (\bar{M}_w) and B) number average (\bar{M}_n) molecular weights of PS-benzophenone based photosensitizer composites under different UV irradiation time*

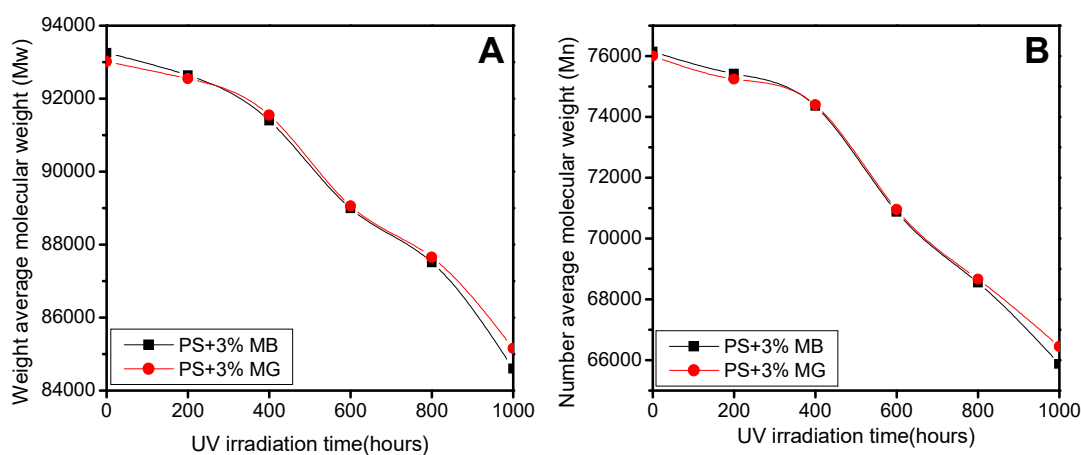


Figure 6.2.2. *A) Weight average (\bar{M}_w) and B) number average (\bar{M}_n) molecular weights of PS-dye composites under different UV irradiation time*

The number of chain scission per molecule (S) and number of scission events per gram (N_t) determined from \bar{M}_n for the PS-benzophenone based photosensitizer composites were found to be maximum for PS-4MOBP and minimum for PS-2HO4MOBP upon UV irradiation (Figure 6.2.3). The values of S and N_t of PS-MB

were slightly higher than that of PS-MG among PS-dye photosensitizer composites upon UV irradiation (Figure 6.2.4).

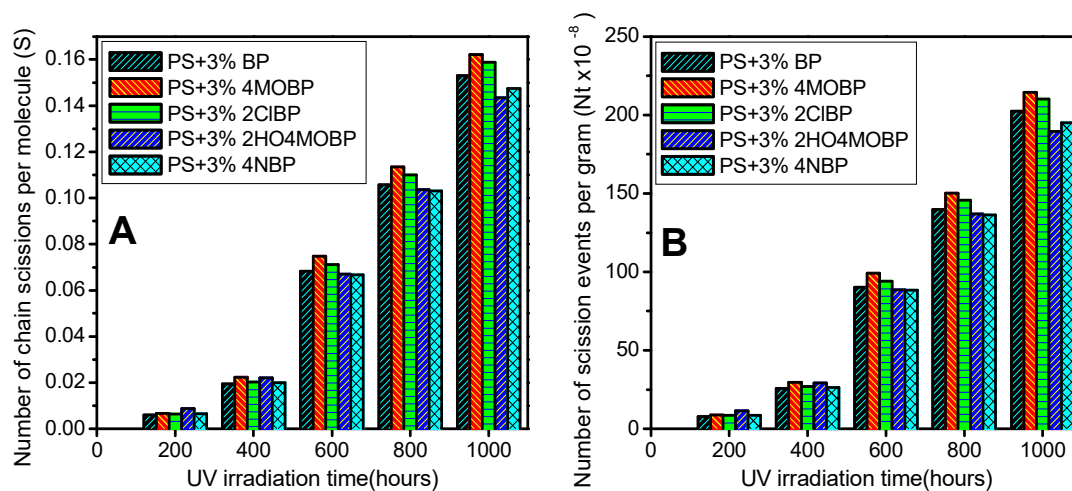


Figure 6.2.3. *A) Number of chain scissions per molecule (S) and B) number of scission events per gram (N_t) of PS-benzophenone based photosensitizer composites under different UV irradiation time intervals*

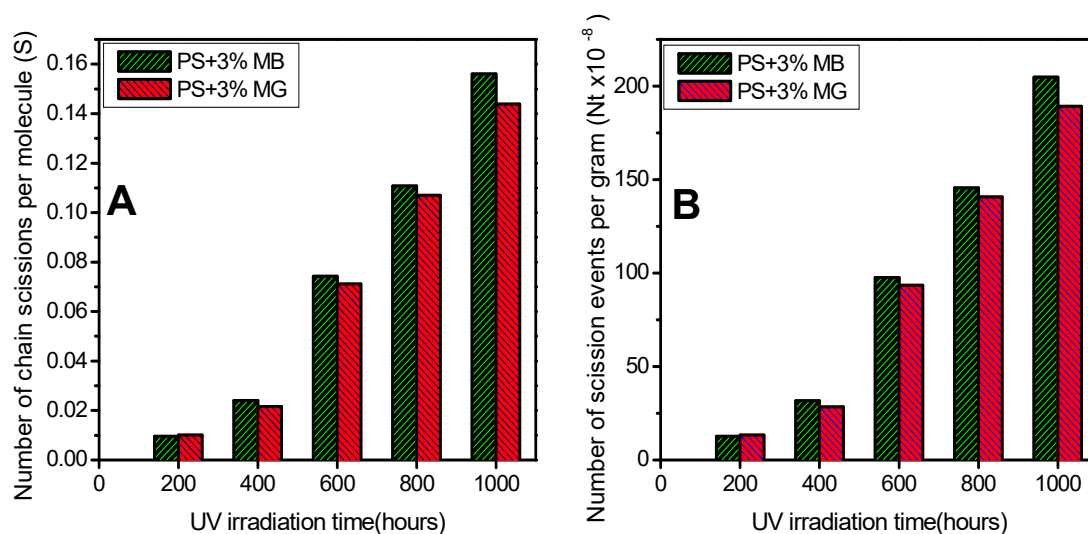


Figure 6.2.4. *A) Number of chain scissions per molecule (S) and B) number of scission events per gram (N_t) of PS- dye photosensitizer composites under different UV irradiation time intervals*

Polydispersity index (PDI) of all the PS composites increased as the time of UV irradiation increased (Figure 6.2.5). The increase in chain scission in random manner due to photodegradation was evident here.

From the GPC data, maximum chain scission, as well as maximum decrease in the average molecular mass was observed in PS-4MOBP composite among the PS-

benzophenone based composites. It was also noted that various substituents on benzophenone altered the rate of chain scission of the PS matrix to which they are loaded. Among the PS-dye composites, PS-MB exhibited maximum chain cleavage and decrease in average molecular mass compared to PS-MG.

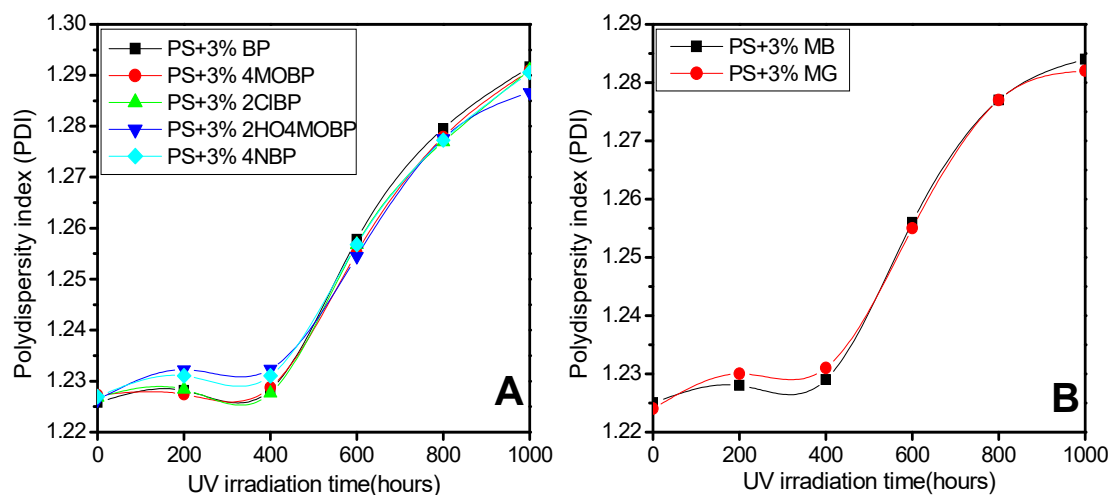


Figure 6.2.5. Polydispersity index (PDI) of PS–benzophenone based and PS–dye photosensitizer composites, under different UV irradiation time.

6.2.2. FTIR Spectroscopy

The FTIR spectra of the PS composites displayed all the bands corresponding to the stretching vibrations of PS as well as the photosensitizers loaded into it (Figure 6.3). The bands at $1740\text{--}1700\text{ cm}^{-1}$ observed in all the PS-benzophenone based photosensitizer composites before UV irradiation attributed to $>\text{C}=\text{O}$ stretching vibrations of benzophenone moiety. Even though only 2HO4MOBP contains $-\text{OH}$ group, the spectra of all PS-benzophenone based photosensitizer composites exhibited bands corresponding to $-\text{OH}$ ($3700\text{--}3600\text{ cm}^{-1}$) before UV irradiation. This could be due to the enolic form of benzophenone moiety existing in the composites or could be due to the adsorbed water from the atmosphere. As the time of UV irradiation increased, an increase in the bands corresponding to $>\text{C}=\text{O}$ and $-\text{OH}$ or $-\text{OOH}$ was observed suggesting photo-oxidation of PS chain. A striking observation for all PS-benzophenone based photosensitizer composites was that increase in the intensity of the bands between 1700 and 1650 cm^{-1} ($>\text{C}=\text{C}<$ stretching) was a little more than that of the bands between 1740 and 1700 cm^{-1} ($>\text{C}=\text{O}$ stretching). This observation supports the fact that the formation of alkenic double bonds over the PS chain took place much effectively than the formation of carbonyl bonds for PS-benzophenone

based photosensitizer composites upon UV irradiation. In the coming section (section 6.5), the possible reason for this observation is explained through suitable mechanism. An increase in the band intensities corresponding to conjugated carbon-carbon double bonds were also observed at around 1600 cm^{-1} . The yellowing of the composites upon UV exposure was a visual support to the conjugated double bond formation which is further supported by the UV-visible spectroscopy to be discussed shortly.

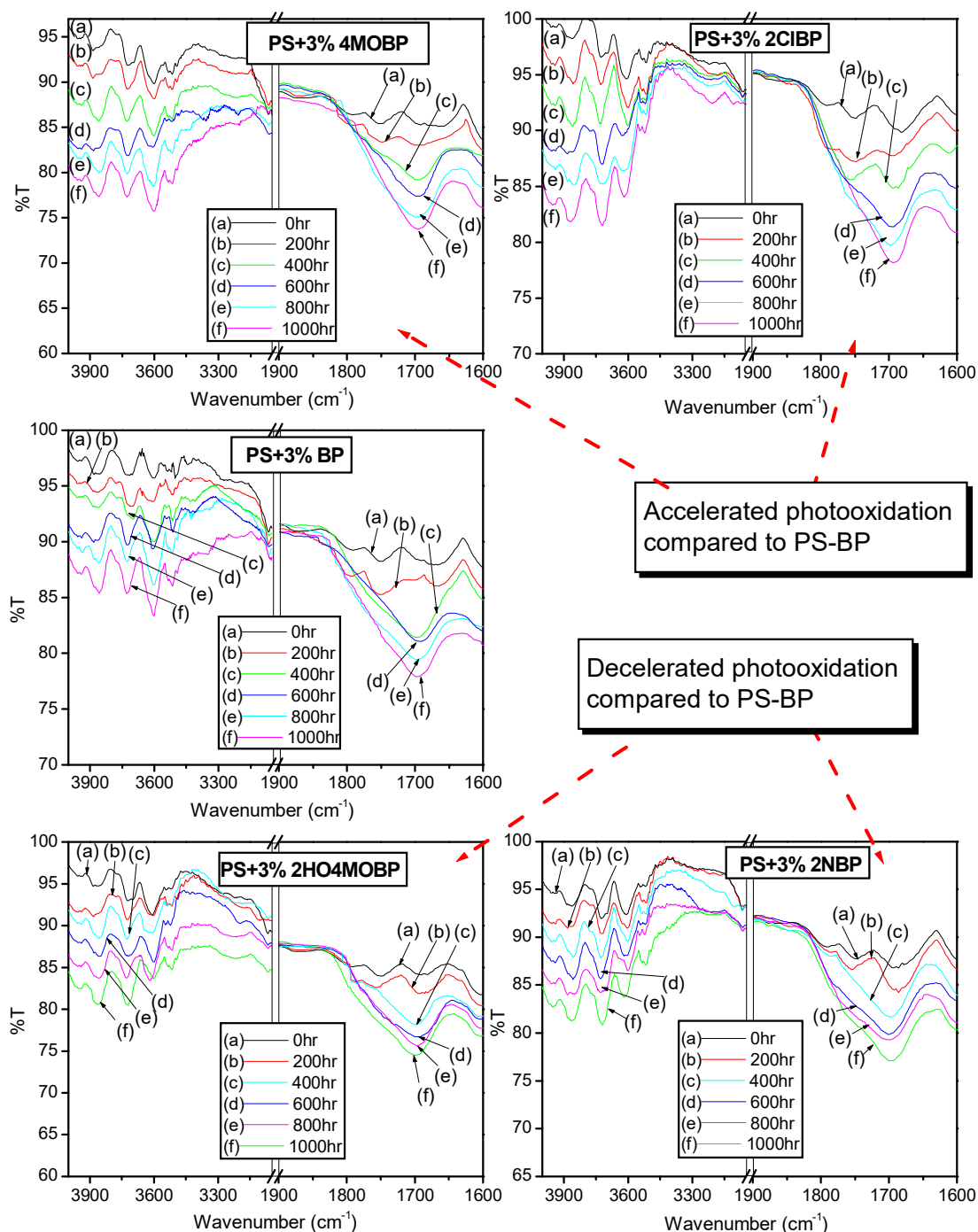


Figure 6.3. FTIR spectra of PS-benzophenone based photosensitizer composites at different UV exposure time intervals ranging from 0 h to 1000 h.

Bands observed at around 690, 750, 905 and 1025 cm^{-1} attributing -C-H out of plane bending of the phenyl rings. The peaks at around 1448 cm^{-1} was unaltered upon UV irradiation. This observation supports the fact that the phenyl rings of PS matrix remained unaltered upon UV irradiation of 1000 hours. In addition to this we could also arrive into a possible conclusion that the phenyl rings of benzophenone derivatives used as photosensitizers too remained without much degradation.

Maximum photo-oxidation was observed in PS-4MOBP followed by PS-2CIBP composites and minimum photo-oxidation was observed in PS-2HO4MOBP among the PS-benzophenone based photosensitizer composites. The extent of photo-oxidation of the PS-photosensitizer composites was however lower compared to PS-TiO₂ composite.

Observations made from the FTIR spectra after UV irradiation of the PS-dye photosensitizer composites were entirely different from that of PS-benzophenone based photosensitizer composites. Much acceleration in the photodegradation was not observed in PS-MB and PS-MG composites under UV radiation. The increase in the absorption band intensities corresponding to $>\text{C}=\text{O}$, $-\text{OH}$, $>\text{C}=\text{C}<$ etc was not in accordance with UV irradiation time. The random increase in the bands of these functional groups upon UV irradiation suggested the possibility of degradation/reactions occurring on the organic dyes themselves. Randomness in the FTIR spectra upon UV irradiation made it difficult to draw a conclusion regarding the photo-oxidation on PS chains.

6.2.3. UV- visible diffused reflectance spectroscopy (UV-DRS)

UV-DRS of PS-benzophenone based photosensitizer composites showed that their prominent absorption is in the UV region (Figure 6.4.1). Since PS as well as benzophenone derivatives had their absorption maxima in the UV region, their composites gave rise to broad band between 200-400 nm. The absorptions in the visible region were almost absent. The intensity of absorption bands between 200-400 nm in all the PS-benzophenone based photosensitizers decreased as the time of UV irradiation increased. This observed trend supported photodegradation. In addition to the decrease in the intensity of absorption bands between 200-400 nm, bathochromic shifts were also observed in the composites upon UV irradiation. Maximum decrease

in the band intensity was observed in the PS-4MOBP composites followed by PS-2ClBP and the minimum decrease was observed in PS-2HO4MOBP among PS-benzophenone based composites.

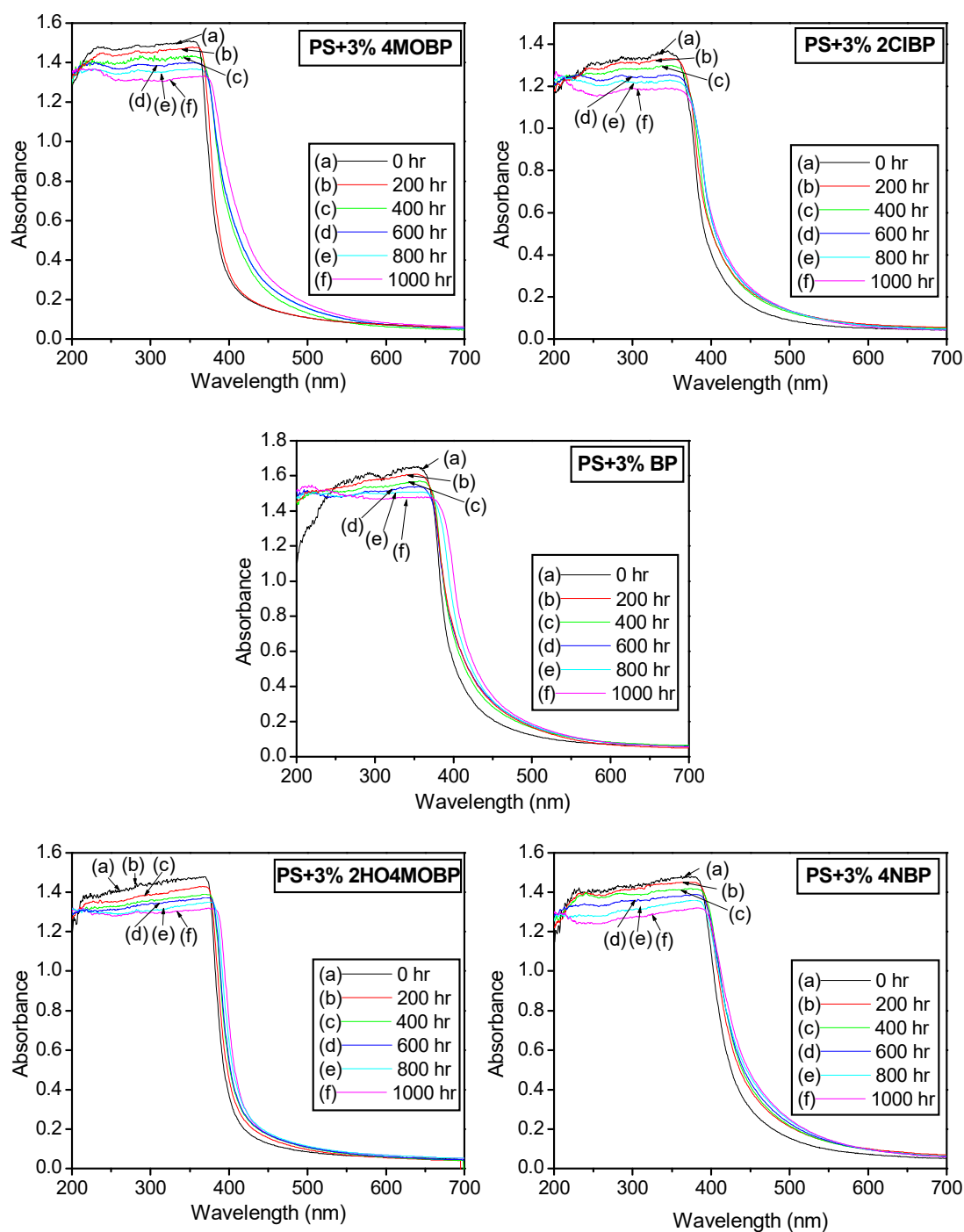


Figure 6.4.1. UV-DRS of PS-benzophenone based photosensitizer composites at regular UV irradiation time intervals

UV-DRS of PS-dye photosensitizer composites displayed absorption bands in the UV as well as visible region of the spectra (Figure 6.4.2). PS-MB composites

exhibited absorption band with λ_{\max} at 273 nm ($\pi \rightarrow \pi^*$). A shoulder peak was observed at around 322 nm. Another less intense broad band was observed between 368 nm and 442 nm ($n \rightarrow \pi^*$). A broad absorption band starting from 457 nm with λ_{\max} at around 600 nm was also observed in the visible region ($n \rightarrow \pi^*$). A sudden change in the shape of absorption bands were noticed even after 200 hours of UV irradiation of PS-MB composite. The shoulder peak observed at around 300 nm was completely masked by a new band between 200 to 350 nm in the UV irradiated composites. Upon UV exposure for 200 hours, the intensity of broad band observed in the visible region with λ_{\max} at around 600 nm had decreased considerably. On further UV exposure, the intensity of absorption bands in the UV region decreased with a red shift. The intensity of the broad bands in visible region observed, decreases gradually up to the measured region. The decrease in intensity of bands observed in the visible region could be due to the change in chemical structure or degradation of MB itself. The quinonoid part of the dye might have transformed into benzenoid structure as a result of UV irradiation leading to its decolouration. The decrease in the intensity of bands observed in the UV region could be due to the degradation of PS as well as MB.

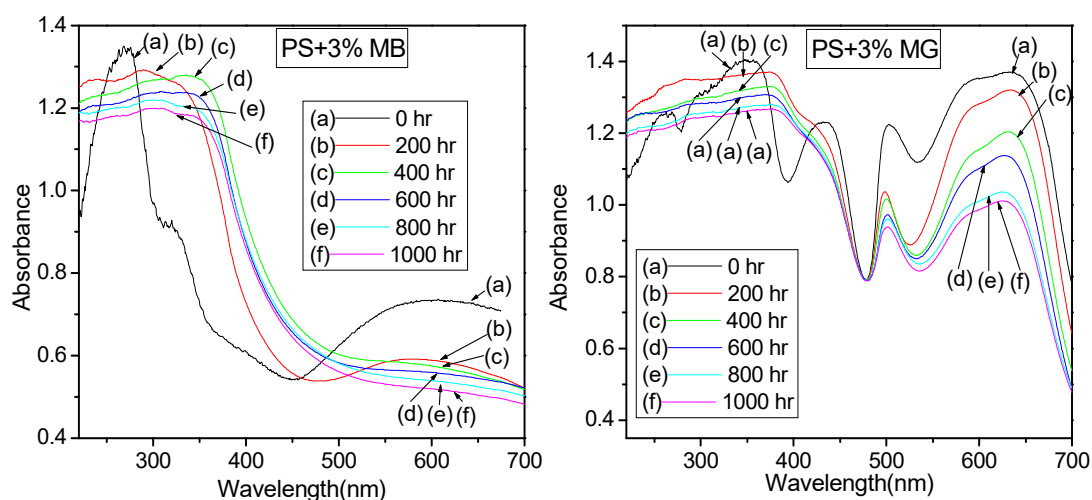


Figure 6.4.2. UV-DRS of PS- dye composites at regular UV irradiation time intervals

The absorption bands of PS-MG composites (Figure 6.4.2) were observed at 263 nm and 348 nm (highest intensity) with a shoulder peak at 303 nm ($\pi \rightarrow \pi^*$) in the UV region. Another band extended from UV region to visible region having λ_{\max} at 433 nm ($n \rightarrow \pi^*$). The bands observed in the visible region at 502 nm and 634 nm (broad high intense band) with a shoulder peak at 594 nm were of high intensity. UV irradiation of PS-MG composites resulted in rearrangement of peak positions and

intensities. As observed in the case of PS-MB composites, the bands at the UV region of PS-MG composites too transformed into broader bands between 200-400 nm masking the peak at 263 nm upon UV irradiation. The band at 433 nm remained as shoulder of the broad band between 200-400 nm even after UV irradiation. A decrease in the intensity of absorption bands in the UV region of PS-MG composites were observed upon UV irradiation. This could be due to the degradation of PS and MG. Decrease in the intensity of the bands in the visible region was also observed upon UV irradiation. This could be due to the degradation/ structural change of MG dye on UV irradiation.

6.2.4. Mechanical properties

The mechanical (flexural and tensile) properties of non-irradiated PS-benzophenone based photosensitizer and PS-dye composites almost looked similar except for a lower value observed in PS-MG composite compared to others (Figure 6.5.1). This observed decrease in the mechanical properties could be due to small aggregation of MG formed within the PS composites affecting its uniform dispersion up to an extent.

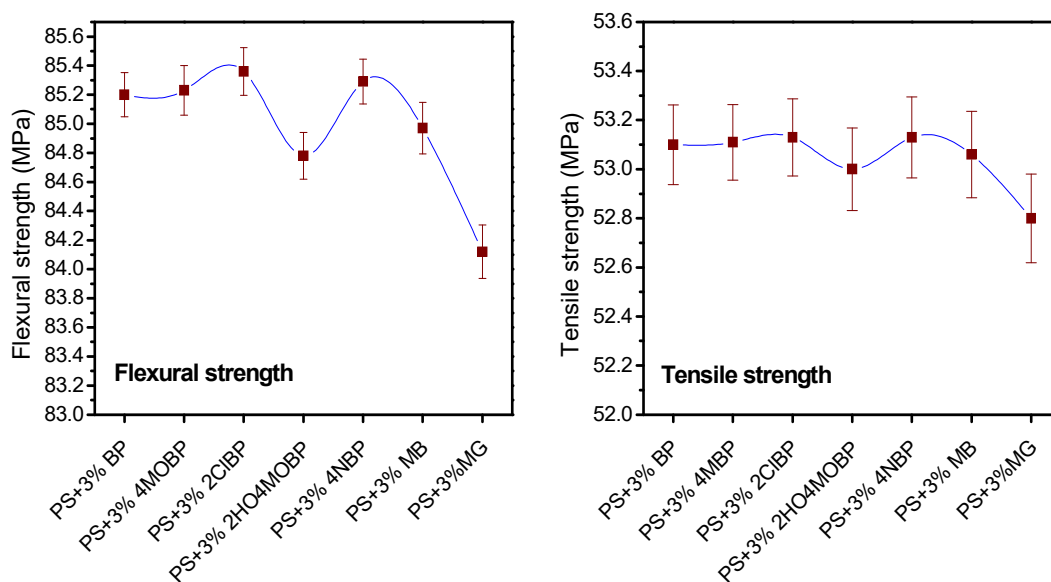


Figure 6.5.1. Flexural (A) and tensile (B) strengths of PS-benzophenone based photosensitizer and PS-dye composites before UV irradiation-a comparison

Plots of mechanical properties of PS-benzophenone based and PS-dye composites with respect to UV irradiation of 0, 400 and 1000 hours are presented in figure 6.5.2.

Out of the PS-benzophenone based photosensitizer composites, PS-3% 4MOBP (which exhibited maximum degradation) and PS-3% 2HO4MOBP (which exhibited minimum degradation) were chosen for mechanical testing. The mechanical properties of PS-3% MG and PS-3% MB were also tested. Figure 6.5.2 shows that the mechanical properties of all the composites decreased upon UV irradiation. PS-4MOBP composite underwent more mechanical deterioration compared to PS-2HO4MOBP as expected. The mechanical properties of PS-dye composites were not as expected. Even though we have noticed that PS-MB composite underwent better photodegradation compared to PS-MG composite, a decrease in the flexural and tensile strength of PS-MB was less compared to PS-MG. The possible reason for such an anomalous trend could be the poor dispersion of MG compared to MB in the PS matrix. The slight aggregation of MG along the PS matrix might have weakened the mechanical strengths of PS-MG composite.

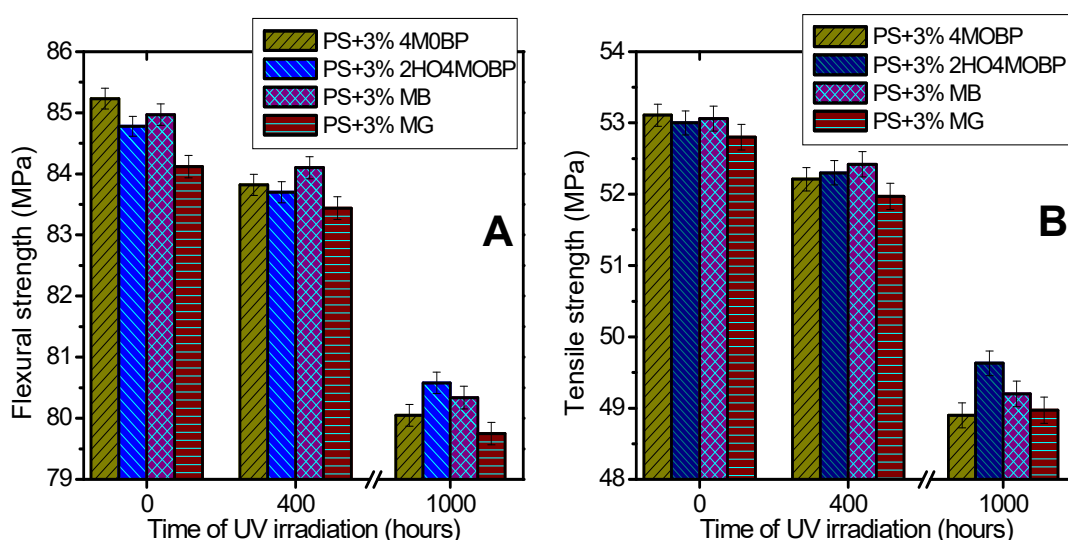


Figure 6.5.2. Flexural (A) and tensile (B) strengths of PS-benzophenone based and PS-dye composites exposed to UV radiation for 0, 400 and 1000 h

6.2.5. Electrical properties

Breakdown voltage (BDV) of PS-3% 4MOBP and PS-3% 2CIBP which underwent better photodegradation among the PS-benzophenone based photosensitizer composites and PS-3% MB which underwent better degradation among the PS-dye composites were measured at UV irradiation time intervals 0, 400 and 1000 hours (Figure 6.6.1). A decrease in the BDV of the composites with respect to UV irradiation time was observed. The extent of decrease in the values of BDV

was found to be better for PS-3% 2CIBP compared to that of PS-3% 4MOBP composite even though the later underwent better photodegradation compared to PS-3% 2CIBP. This observed decrease in BDV upon photodegradation could be due to the formation of more current conducting charge carriers in PS-3% 2CIBP compared to PS-3% 4MOBP on UV exposure.

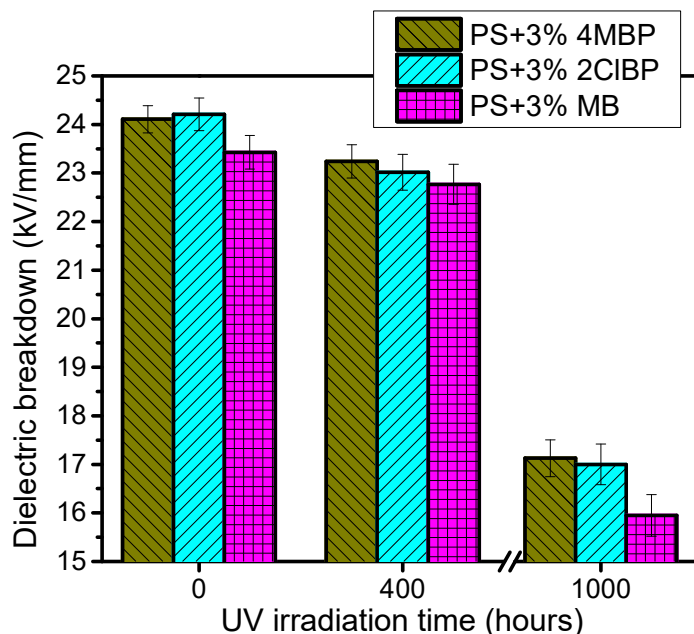


Figure 6.6.1. Dielectric breakdown (breakdown voltage) of PS-4MOBP, PS-2CIBP and PS-MB composites with varying UV irradiation time

Dielectric permittivity (ϵ_r) of PS-3% 4MOBP, PS-3% 2CIBP among the PS-photosensitizer composites (Figure 6.6.2) and PS-3% MB and PS-3% MG among PS-dye composites (Figure 6.6.3) were measured at UV irradiation time intervals of 0, 400 and 1000 hours. The ϵ_r of all the composites increased as the time of UV irradiation is increased. Formation of charged polar species on UV exposure of the samples as a result of photodegradation was hence evident. PS-3% 2CIBP underwent better increase in ϵ_r compared to PS-3% 4MOBP as the time of UV irradiation increased. This shows that better charged dipoles may be found in UV irradiated PS-3% 2CIBP compared to that of PS-3% 4MOBP. For the PS-dye system, PS-3% MB exhibited better decrease in the value of ϵ_r compared to PS-3% MG upon UV irradiation.

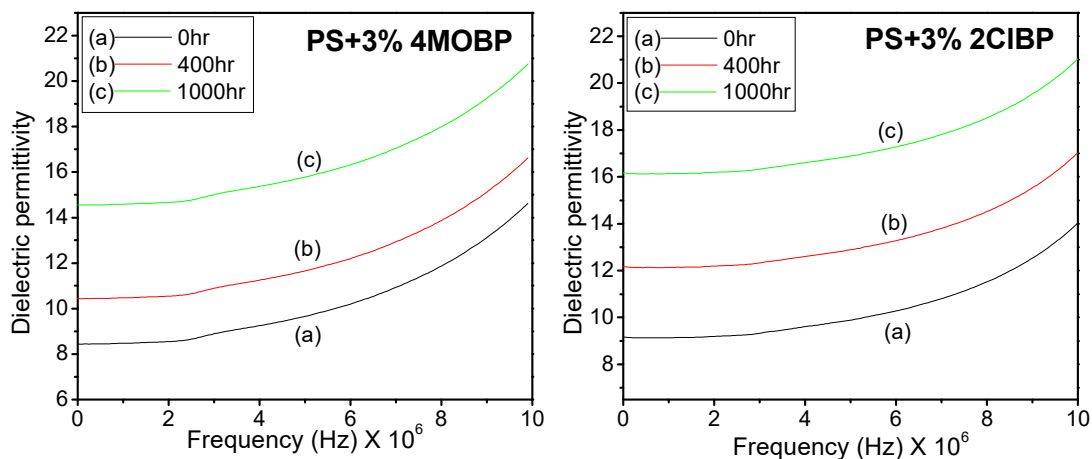


Figure 6.6.2. Dielectric permittivity of PS-3% 4MOBP and PS-3% 2CIBP composites at UV irradiation intervals of 0 h, 400 h and 1000 h.

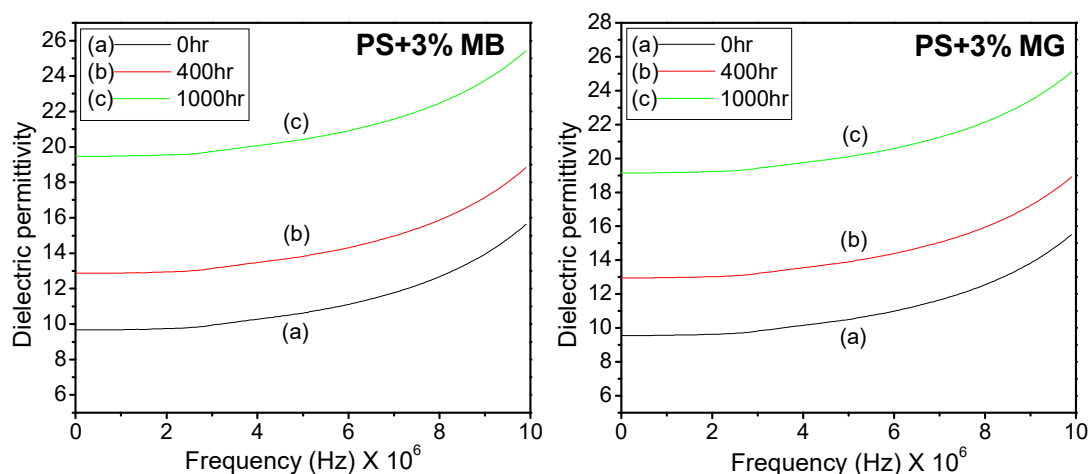


Figure 6.6.3. Dielectric permittivity of PS-3% MB and PS-3% MG composites at UV irradiation intervals of 0 h, 400 h and 1000 h.

6.2.6. Thermogravimetric Analysis (TGA)

The TGA of PS-3% 4MOBP (Figure 6.7 A) and PS-3% MB (Figure 6.7 B) which underwent maximum photodegradation among the PS-benzophenone based photosensitizer and PS-dye photosensitizer composites respectively were conducted under nitrogen atmosphere. The thermogram of both the composites looked alike with two stages of weight losses. The first stage of weight loss attributed to the water desorption process and the second stage of weight loss represents the decomposition of the composites. The decomposition temperature range for PS-3% 4MOBP and PS-3% MB was 264-404°C and 269-408°C respectively. In both the composites the

decomposition shifted to lower temperature range after UV irradiation. The decomposition temperature range for PS-3% 4MOBP was shifted to 252-392°C and that of PS-3% MB to 260-399°C upon UV irradiation of 1000 hours. The decrease in the thermal property of the composites as a consequence of photodegradation on UV exposure was hence concluded from this observation. Sharp decrease in the decomposition peaks terminated at around 404°C (weight percent=4.16%) for PS-3% 4MOBP beyond which the decrease in weight percentage was too slow. Similar observation was made for PS-3% MB beyond 408°C (weight percent=4.2%). The termination point of steep decomposition curve of both the composites shifted to lower values upon UV exposure of 1000 hours.

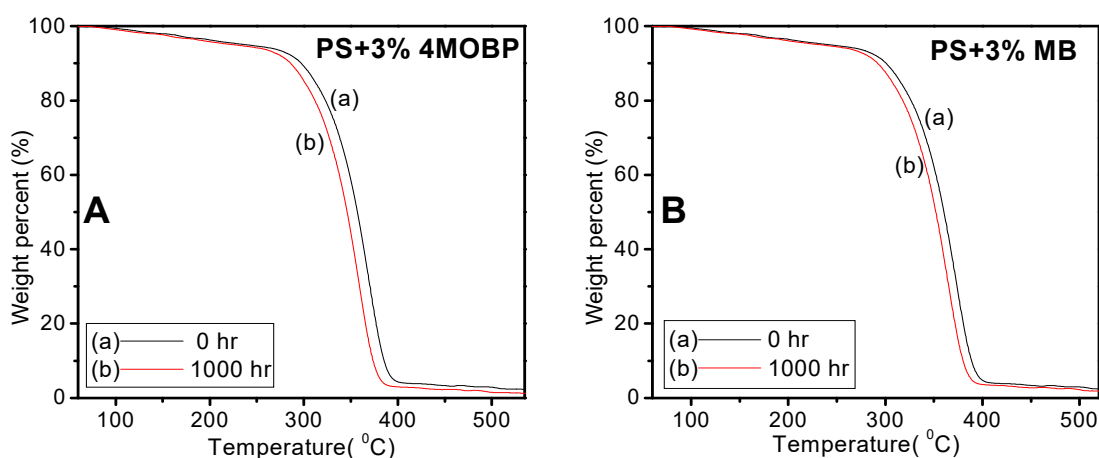


Figure 6.7. TGA thermogram of PS-3% 4MOBP (A) and PS-3% MB (B) composites before and after UV irradiation of 1000 h

6.2.7. Weight loss

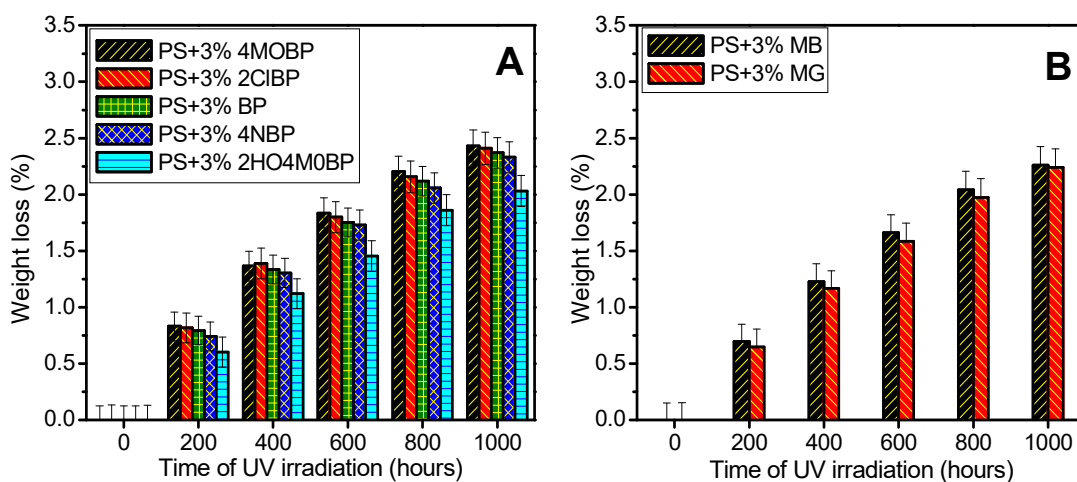


Figure 6.8. Comparison of weight loss percentages of PS-3% benzophenone based photosensitizer (A) and PS-3% dye (B) composites at regular intervals of UV irradiation

Weight loss was observed in all the PS-benzophenone based photosensitizer composites (Figure 6.8 A) as well as PS-dye composites (Figure 6.8 B) as the time of UV irradiation of the samples increased. The weight loss percentage of the PS-benzophenone based composites followed the order:- PS-3% 4MOBP > PS-3% 2CIBP > PS-3% BP > PS-3% 4NBP > PS-3% 2HO4MOBP. The weight loss percentage of PS-dye composites followed the following order: - PS-3% MB > PS-3% MG.

Section:II

Enhanced photocatalytic activity of nano TiO₂ coupled benzophenone derivatives and organic dyes for the UV degradation of polystyrene

6.3. Preparation of PS-TiO₂ -photosensitizer composites

Three sets of PS-TiO₂-benzophenone based photosensitizer composites were prepared as described in chapter 2. In the first set, the mole percentage of benzophenone based photosensitizers were 50% of nano TiO₂. In the second set, the mole percentage of TiO₂ and benzophenone based photosensitizers were of equal mole percentage. In the third set, nano TiO₂ was 50 mole percentage of benzophenone based photosensitizers. All these composites were 3% by weight of PS.

The prepared combinations of PS-TiO₂-dye photosensitizer were much different from that of PS-TiO₂-benzophenone based photosensitizer composites. In this case, better efficiency among the nano TiO₂-dye composites were observed at low mole percentage of the dye. Better degradation efficiency was observed when the mole percentage of dyes was 5% of nano TiO₂. This optimisation in the percentage of dyes was done by comparing the photodegradation of PS using nano TiO₂-dye composites where the mole percentages of the dyes were varied from 0.5% to 10% of nano TiO₂.

The tables below describe in detail, the composition of the PS-TiO₂-benzophenone based photosensitizer and PS-TiO₂-dye photosensitizer composites prepared in our study for the photodegradation of PS.

Table 6.2.1. PS-TiO₂-benzophenone based photosensitizer composites

PS+3% (TiO₂+50% benzophenone based photosensitizer) composites			
Set 1	<i>Sl no:</i>	<i>Composites</i>	<i>Description</i>
	1	PS+3% (TiO ₂ +50% BP)	<ul style="list-style-type: none"> All the benzophenone based compounds are 50 mole % of nano TiO₂. The TiO₂-50% photosensitizer composites are 3 weight % of PS
	2	PS+3% (TiO ₂ +50% 2HO4MOBP)	
	3	PS+3% (TiO ₂ +50% 4MOBP)	
	4	PS+3% (TiO ₂ +50% 2CIBP)	
	5	PS+3% (TiO ₂ +50% 4NOBP)	
PS+3% (TiO₂+benzophenone based photosensitizer) composites			
Set 2	<i>Sl no</i>	<i>Composites</i>	<i>Description</i>
	1	PS+3% (TiO ₂ +BP)	<ul style="list-style-type: none"> All the benzophenone based compounds and nano TiO₂ are of equal mole % The TiO₂- photosensitizer composites are 3 weight % of PS
	2	PS+3% (TiO ₂ +2HO4MOBP)	
	3	PS+3% (TiO ₂ +4MOBP)	
	4	PS+3% (TiO ₂ +2CIBP)	
	5	PS+3% (TiO ₂ +4NOBP)	
PS+3% (Benzophenone based photosensitizer + 50% TiO₂) composites			
Set 3	<i>Sl no</i>	<i>Composites</i>	<i>Description</i>
	1	PS+3% (BP + 50% TiO ₂)	<ul style="list-style-type: none"> Nano TiO₂ was 50 mole % of benzophenone based compounds The photosensitizer-50% TiO₂ composites are 3 weight % of PS
	2	PS+3% (2HO4MOBP+ 50% TiO ₂)	
	3	PS+3% (4MOBP+ 50% TiO ₂)	
	4	PS+3% (2CIBP+ 50% TiO ₂)	
	5	PS+3% (4NOBP+ 50% TiO ₂)	

Table 6.2.2. PS-TiO₂-dye photosensitizer composite

	<i>Sl no</i>	<i>Composites</i>	<i>Description</i>
Set 1	1	PS+3% (TiO ₂ + 0.5% MB)	<ul style="list-style-type: none"> The dyes are 0.5 mole % of TiO₂ The TiO₂-0.5% dye is 3 weight % of PS
	2	PS+3% (TiO ₂ + 0.5% MG)	
Set 2	1	PS+3% (TiO ₂ + 1% MB)	<ul style="list-style-type: none"> The dyes are 1 mole % of TiO₂ The TiO₂-1% dye is 3 weight % of PS
	2	PS+3% (TiO ₂ + 1% MG)	
Set 3	1	PS+3% (TiO ₂ + 2% MB)	<ul style="list-style-type: none"> The dyes are 2 mole % of TiO₂ The TiO₂-2% dye is 3 weight % of PS
	2	PS+3% (TiO ₂ + 2% MG)	
Set 4	1	PS+3% (TiO ₂ + 3% MB)	<ul style="list-style-type: none"> The dyes are 3 mole % of TiO₂ The TiO₂-3% dye is 3 weight % of PS
	2	PS+3% (TiO ₂ + 3% MG)	

Set 5	1	PS+3% (TiO ₂ + 5% MB)	<ul style="list-style-type: none"> • The dyes are 5 mole % of TiO₂ • The TiO₂-5% dye is 3 weight % of PS
	2	PS+3% (TiO ₂ + 5% MG)	
Set 6	1	PS+3% (TiO ₂ + 7% MB)	<ul style="list-style-type: none"> • The dyes are 7 mole % of TiO₂ • The TiO₂-7% dye is 3 weight % of PS
	2	PS+3% (TiO ₂ + 7% MG)	
Set 7	1	PS+3% (TiO ₂ + 10% MB)	<ul style="list-style-type: none"> • The dyes are 10 mole % of TiO₂ • The TiO₂-10% dye is 3 weight % of PS
	2	PS+3% (TiO ₂ + 10% MG)	

For the preparation of PS-TiO₂-photosensitizer composites, particular mole percentage of the photosensitizers with respect to nano TiO₂ was weighed. Nano TiO₂ and the weighed photosensitizers were mixed. 3 weight percentage of the TiO₂-photosensitizer mixture was loaded into PS as described in chapter 2.

6.4. Results and Discussion

Out of the three sets of PS-TiO₂-benzophenone based photosensitizer, those with equal percentages of TiO₂-benzophenone based photosensitizer combination (table 6.2.1, set 2) showed enhanced degradation as evident from various monitoring techniques used. The composites in which the percentage of TiO₂ was only 50% of benzophenone based photosensitizers (table 6.2.1, set 3) showed comparatively lesser degradation. In the case of TiO₂-dye system, entirely different observations were observed. Enhancement in the photocatalytic activity was observed in nano TiO₂-dye composites as expected. TiO₂-dye composites were efficient only at lower dye percentages for the effective photodegradation of PS. Their efficiency increased upto 5 mole % dyes coupled with TiO₂ (we have studied the photodegradation of PS using various TiO₂-dye combinations having 0.5, 1, 2, 3, 5, 7 and 10 mole % dyes coupled with nano TiO₂). When the percentage of the dyes coupled with nano TiO₂ exceeded 5%, the photocatalytic efficiency of the composites for PS degradation gets reduced. The observations and conclusions made from various analytical techniques are discussed below.

6.4.1. Gel Permeation Chromatography (GPC)

A better decrease in \bar{M}_w and \bar{M}_n was observed in PS-TiO₂-benzophenone based photosensitizer composites as well as PS-TiO₂-dye composites compared to the PS-benzophenone based photosensitizer and PS-dye composites upon UV irradiation. The decrease in average molecular weights was predominant in PS-(TiO₂-4MOBP)

composites followed by PS-(TiO₂-2CIBP) (Figure 6.9.1). Among the PS-TiO₂-organic dye systems, PS-(TiO₂-5% MB) showed maximum decrease in the value of \bar{M}_w and \bar{M}_n compared to PS-(TiO₂-5% MG) (Figure 6.9.2).

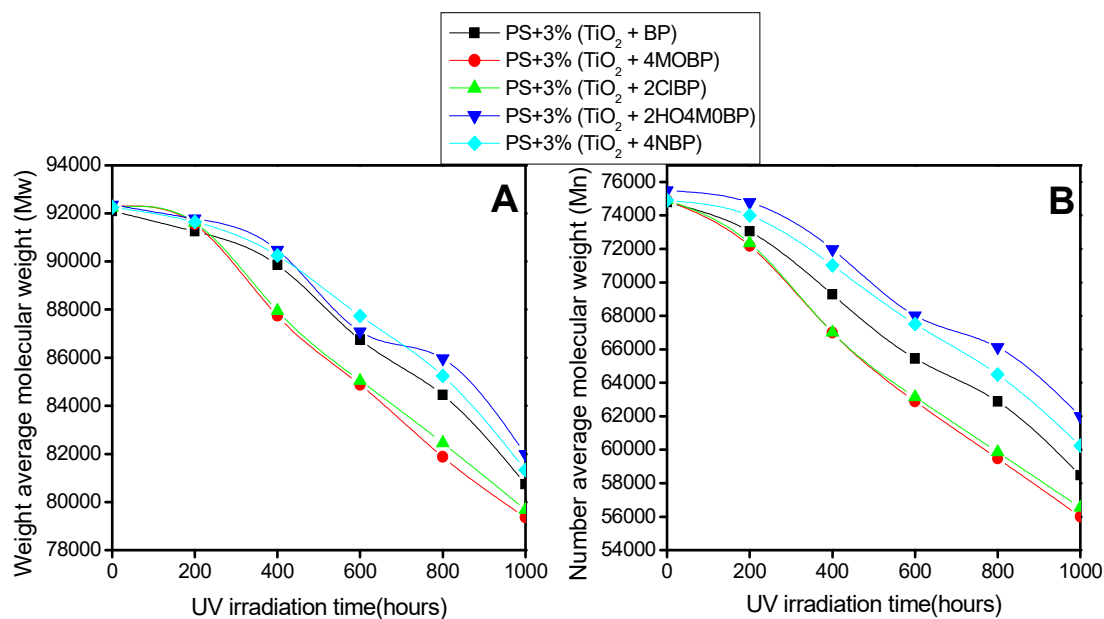


Figure 6.9.1. A) Weight average (\bar{M}_w) and B) number average (\bar{M}_n) molecular weights of PS-TiO₂- benzophenone based photosensitizer composites under different UV irradiation time

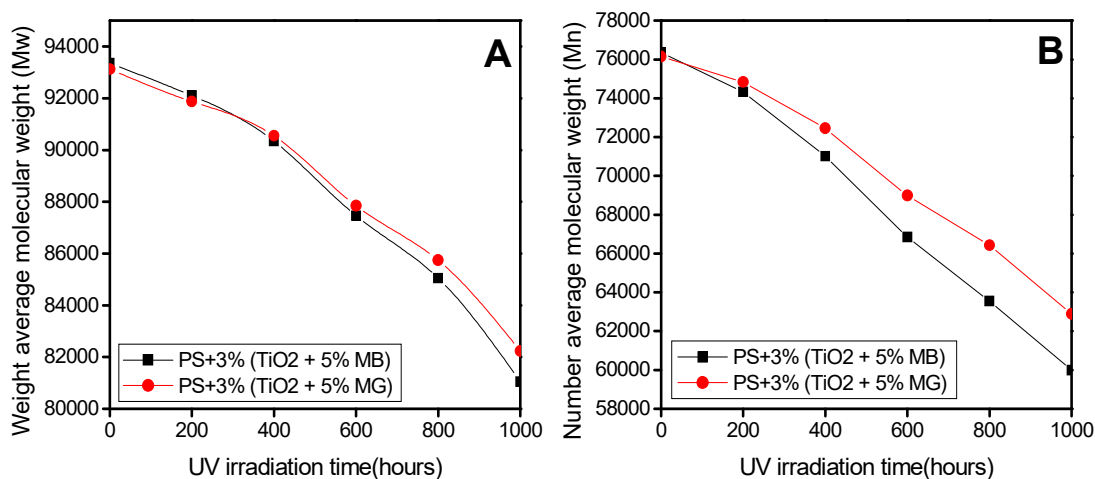


Figure 6.9.2. A) Weight average (\bar{M}_w) and B) number average (\bar{M}_n) molecular weights of PS-TiO₂-dye composites under different UV irradiation time

The plot of number of chain scission per molecule (S) and number of scission events per gram (N_t) versus time of UV irradiation of the composites clearly help us to visualize the variation in chain scission of the composites. It was clear that the polymer chain cleavage occurred more effectively in the PS-(TiO₂-4MOBP) followed

by PS-(TiO₂-2ClBP) among the PS-TiO₂-benzophenone based photosensitizer composites (Figure 6.9.3). The lowest extent of chain scission upon UV irradiation was found to be in PS-(TiO₂-2HO4MOBP) composites. PS-TiO₂-MB underwent better chain scission compared to PS-(TiO₂-MG) among the PS-TiO₂-dye composites (Figure 6.9.4).

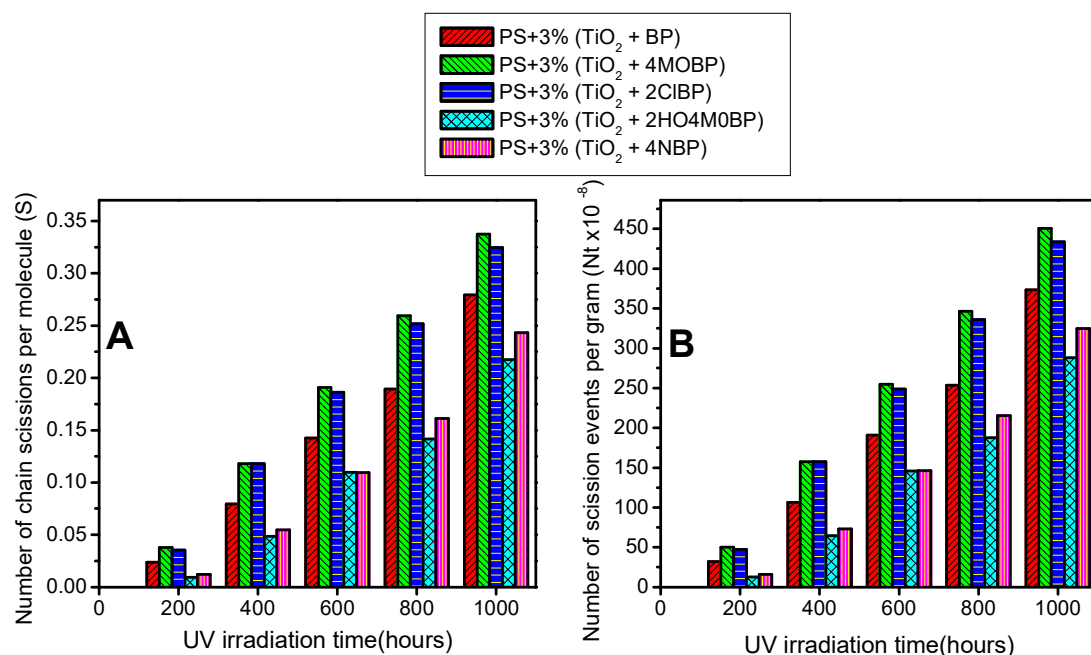


Figure 6.9.3. *A) Number of chain scissions per molecule (S) and B) number of scission events per gram (N_t) of PS-TiO₂-benzophenone based photosensitizer composites under different UV irradiation*

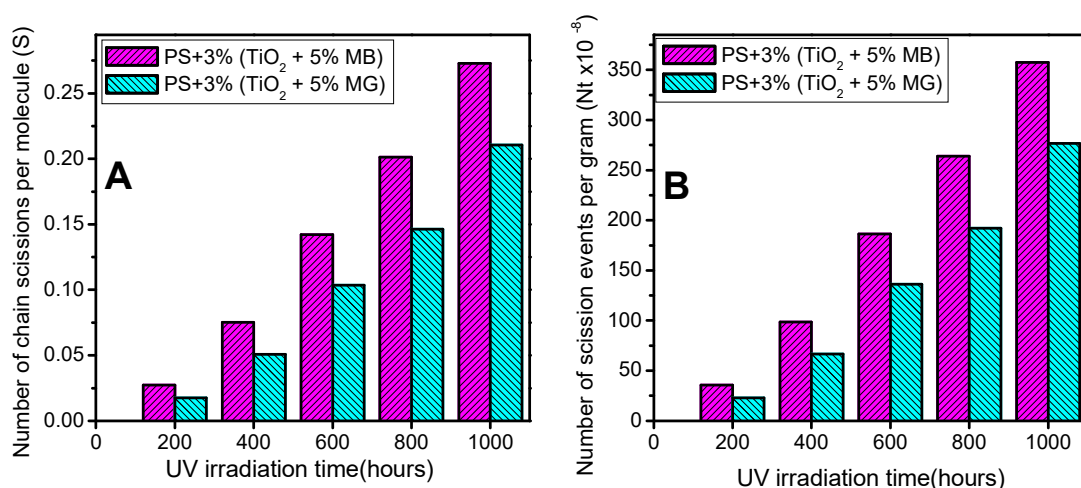


Figure 6.9.4. *A) Number of chain scissions per molecule (S) and B) number of scission events per gram (N_t) of PS-TiO₂-dye composites under different UV irradiation*

The polydispersity index (PDI) increased for all the composites with respect to UV irradiation time. The increase in randomness of chain scission (increase in PDI) was higher for the composites which underwent maximum chain scission upon UV irradiation (Figure 6.9.5). Among the PS-TiO₂-benzophenone based photosensitizer composites, we could see that the PDI of PS-(TiO₂-4MOBP) and PS-(TiO₂-2CIBP) have highest values at each UV irradiation intervals. Among the dye composites, the increase in PDI of PS-(TiO₂-5%MB) composites were better compared to PS-(TiO₂-5%MG).

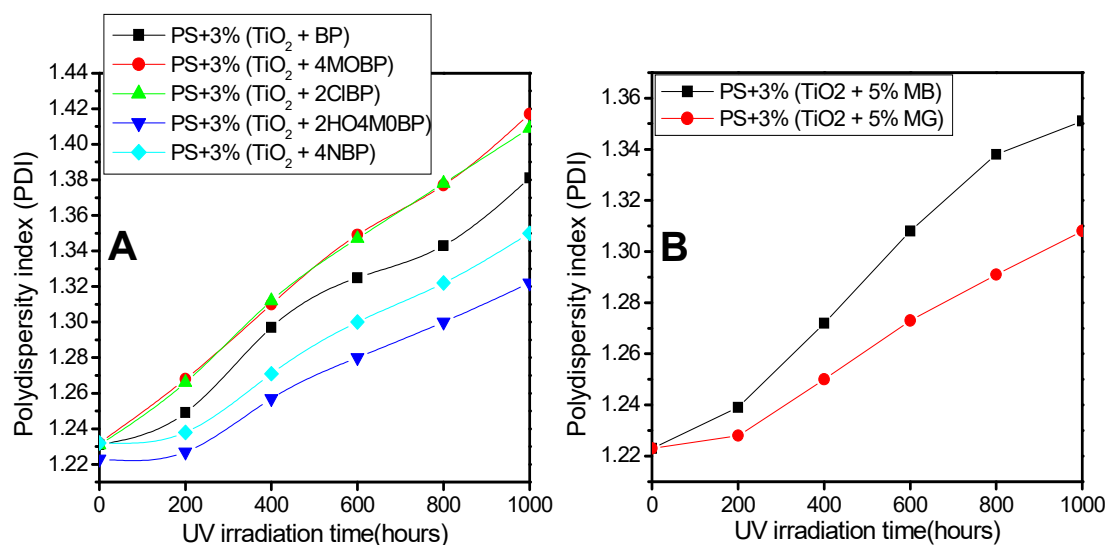


Figure 6.9.5. Polydispersity index (PDI) of PS –TiO₂- benzophenone based photosensitizer and PS-organic dye composite under various UV irradiation times.

6.4.2. FTIR spectroscopy

An appreciable increase in the intensities of absorption bands corresponding to >C=O, -OH/-OOH, >C=C< and conjugated double bonds were observed from the FTIR spectra of PS-TiO₂-benzophenone based photosensitizers upon UV irradiation (Figure 6.10.1). The extent of photo-oxidation of PS-TiO₂-photosensitizer composites was higher compared to PS-benzophenone based photosensitizer as well as PS-TiO₂ composites. PS-(TiO₂-4MOBP) composite underwent maximum photo-oxidation among the PS-TiO₂-benzophenone based photosensitizers followed by PS-(TiO₂-2CIBP). PS-(TiO₂-2HO4MOBP) composite underwent minimum photo-oxidation as expected.

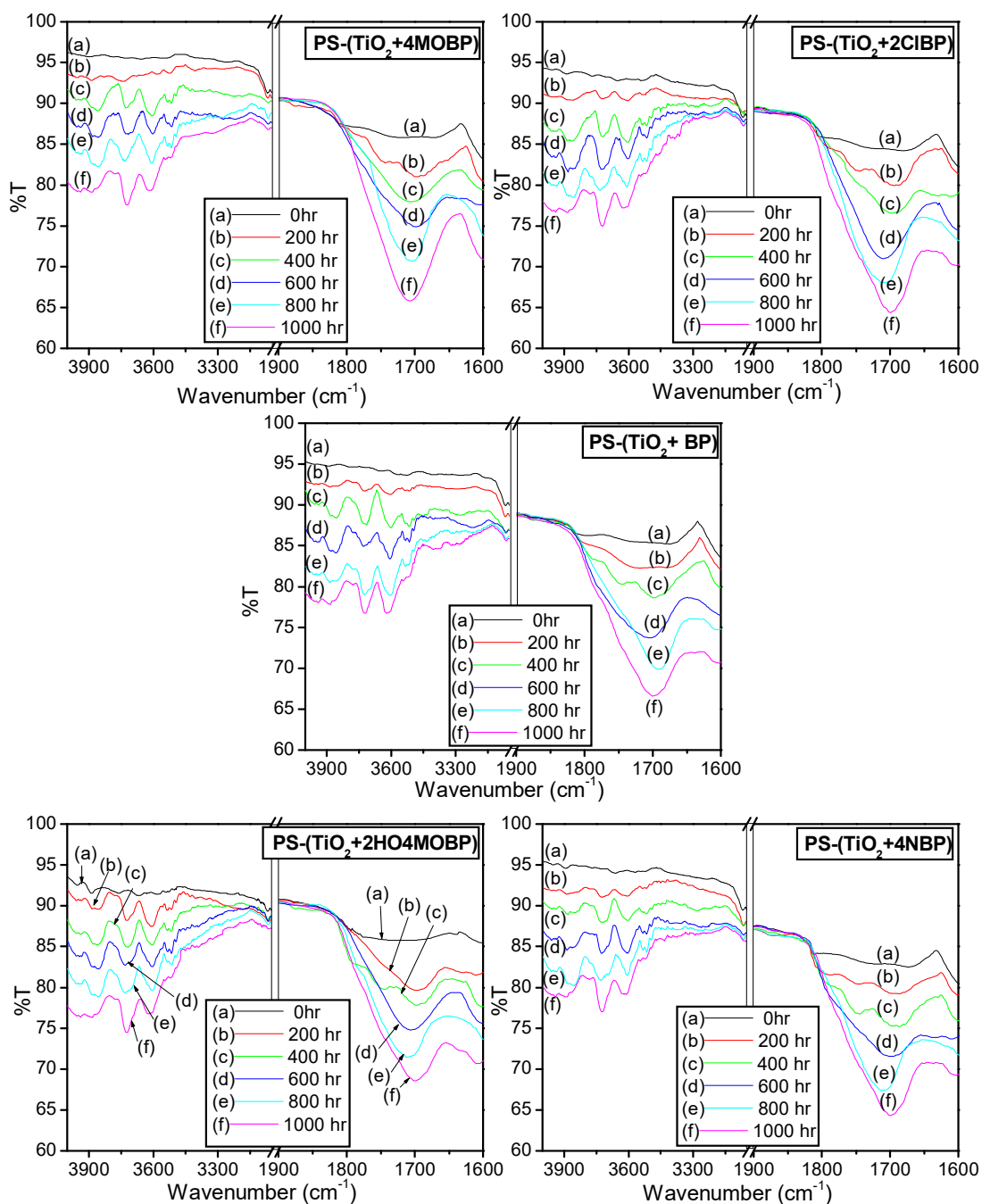


Figure 6.10.1. FTIR spectra of PS-TiO₂-benzophenone based photosensitizer composites at different UV exposure time intervals ranging from 0 h to 1000 h.

We have already seen that for PS-benzophenone based photosensitizer composites, the increase in intensity of absorption bands corresponding to $>C=C<$ stretching vibrations ($1700\text{-}1650\text{ cm}^{-1}$) were more prominent than that of $>C=O$ stretching bands ($1740\text{-}1700\text{ cm}^{-1}$) upon UV irradiation. For PS-TiO₂ composites, the observation was vice versa where the increase in the bands corresponding to $>C=O$ was better than that of $>C=C<$ stretching. In the case of PS-TiO₂-benzophenone based

photosensitizer composites, the extent of increase in the bands corresponding to $>C=O$ as well as $>C=C<$ was equally more appreciable compared to PS-TiO₂ and PS-benzophenone based photosensitizer composites. The contribution of nano TiO₂ and benzophenone based photosensitizers for the photodegradation of PS was hence clear. The increase in the extent of photo-oxidation of these composites compared to PS-TiO₂ as well as PS-benzophenone based photosensitizers also suggests synergic effect of TiO₂ and benzophenone based photosensitizers.

An amazing observation was revealed from the FTIR spectra of PS-TiO₂-dye composites upon UV irradiation (Figure 6.10.2). The photocatalytic activity of nano TiO₂ coupled with organic dyes (MB and MG) increased to an appreciable extent for the photo-oxidation of PS. As already discussed, MG and MB alone were not efficient photocatalysts for the photodegradation of PS. TiO₂ coupled with these dyes acts as a good photocatalyst for PS degradation. Also, it was observed that the extent of photo-oxidation of the PS-TiO₂-dye composites were higher than that of PS-TiO₂ composites. This reveals the fact that MG and MB enhanced the photocatalytic activity of nano TiO₂ for the photodegradation of PS. It was also found that the photo-oxidation of PS-MB composite was higher than that of PS-MG composite.

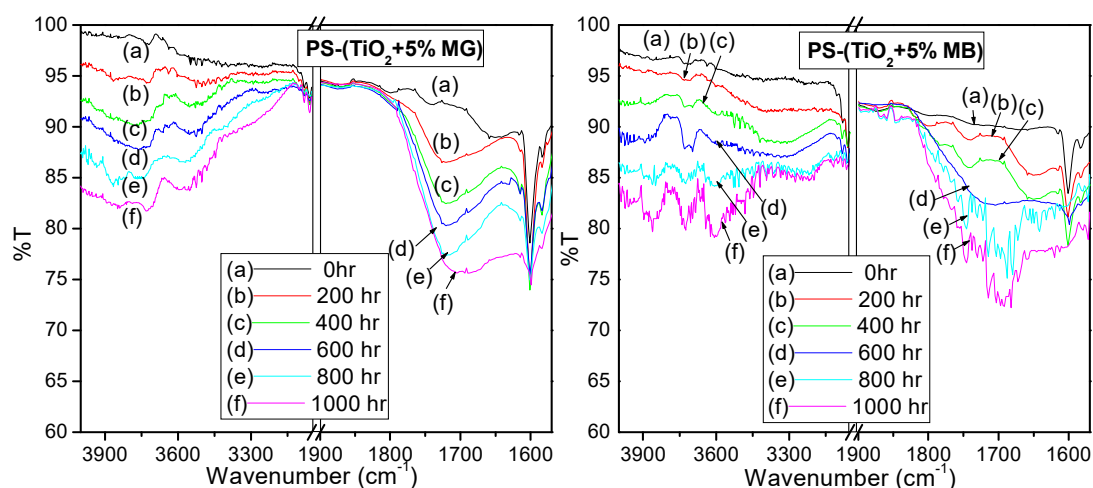


Figure 6.10.2. FTIR spectra of PS-TiO₂- benzophenone based photosensitizer composites at different UV exposure time intervals ranging from 0 h to 1000 h.

6.4.3. UV-visible diffused reflectance spectroscopy (UV-DRS)

Nano TiO₂-photosensitizer incorporated into PS matrix resulted in an appreciable decrease in the absorption bands observed in the UV region of the composites as observed in UV-DRS (Figure 6.11.1). The decrease in absorption bands suggests

photodegradation of PS-TiO₂-benzophenone based photosensitizer composites were higher than that of PS-benzophenone based photosensitizer and PS-TiO₂ composites discussed earlier. PS-TiO₂-4MOBP followed by PS-TiO₂-2ClBP composites underwent maximum decrease in the absorption bands upon UV irradiation. Minimum decrease in the absorption bands upon UV irradiation was observed for PS-TiO₂-2HO4MOBP.

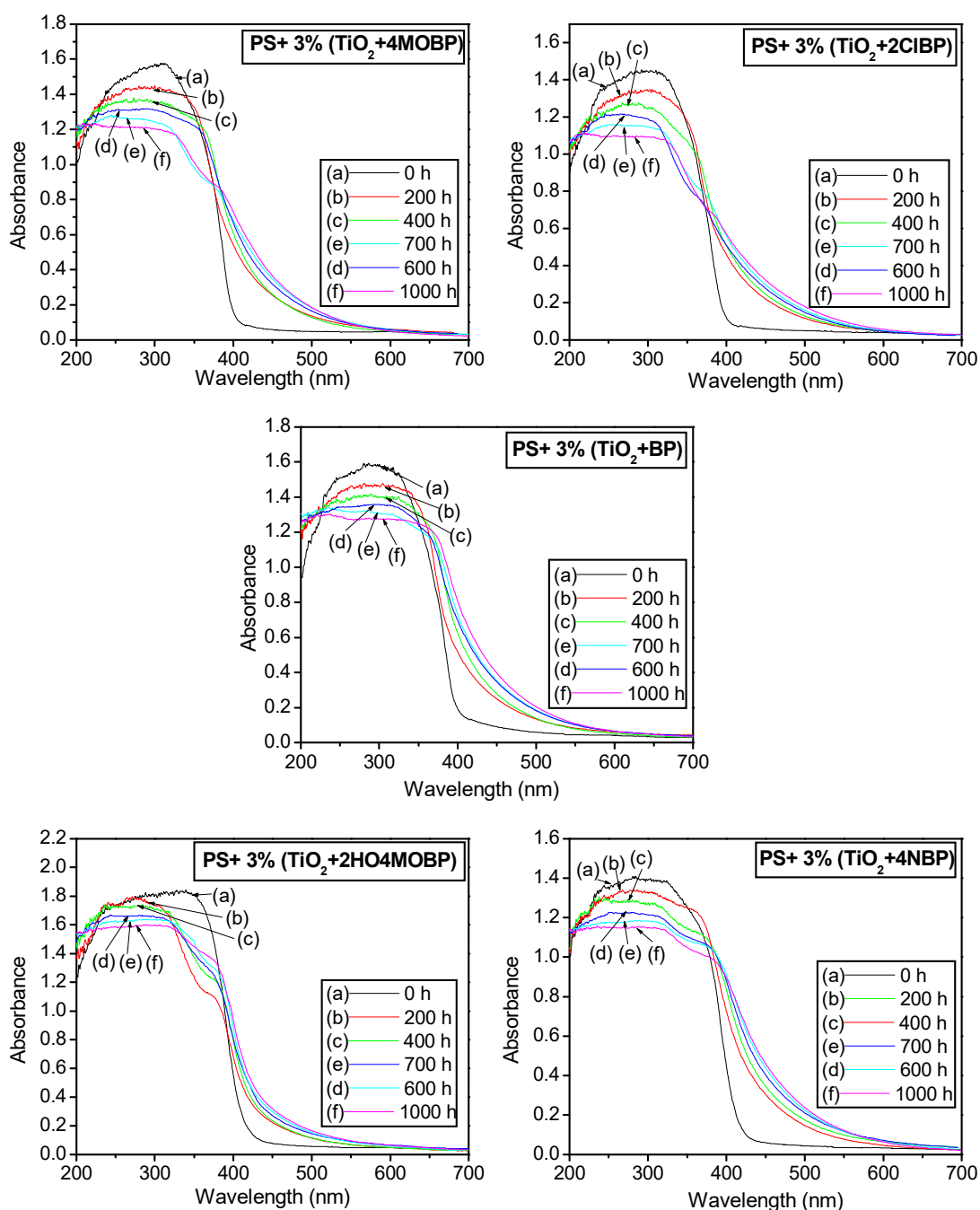


Figure 6.11.1. UV-DRS of PS-TiO₂-benzophenone based photosensitizer composites with UV irradiation time intervals

UV-DRS of PS-TiO₂-MB (Figure 6.11.2) composite looked different from that of PS-MB. The multiple bands observed in the UV region of the spectra for PS-MB was reconstructed into a single band resembling the UV region of the spectra of PS-TiO₂. Multiple bands observed in the visible region of PS-MB were also reconstructed entirely into a long tale like band in PS-TiO₂-MB composite extending to the far-red region. The interaction of nano TiO₂ with MB might have resulted in this peak tailing. The UV region of the UV-DRS of PS-TiO₂-MG on the other hand was similar to that of PS-MG composite (Figure 6.11.2). The visible region of PS-TiO₂-MG is reconstructed into a single broad band compared to the multiple peaks of PS-MG composites discussed above. The changes observed in the visible region of the spectra might have been an outcome of the interaction between nano TiO₂ and MG.

The increase in degradation efficiency of PS-TiO₂-BP, PS-TiO₂-4MOBP, PS-TiO₂-2HO4MOBP, PS-TiO₂-2ClBP and PS-TiO₂-4NBP with respect to pristine PS were 9.87, 13.41, 3.53, 14.53 and 8.25 respectively.

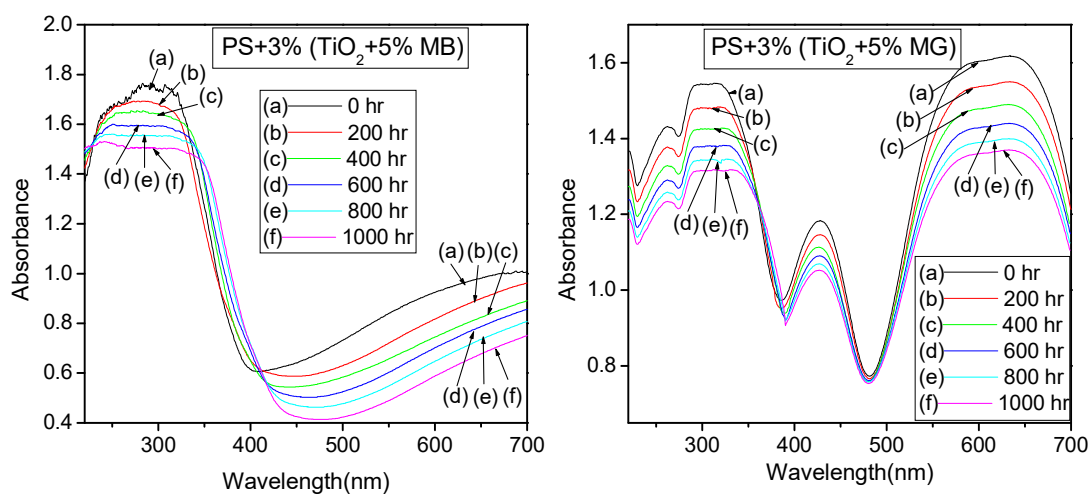


Figure 6.11.2. UV-DRS of PS-TiO₂-dye composites at regular UV irradiation time intervals

A considerable decrease in the absorption bands were observed in PS-TiO₂-MB as well as PS-TiO₂-MG composites upon UV irradiation. Slight bathochromic shift was also noticed for the bands in the UV region of the composites upon UV irradiation. The decrease in the absorption bands in the visible region supports photodegradation of PS as well as the organic dye. It could however be seen that the degradation of dye in the PS-TiO₂-dye composites was not as severe as that observed in PS-dye composites. The decrease in the absorption band intensities upon UV irradiation

observed in PS-TiO₂-dyes was higher compared to that of PS-dye as well as PS-TiO₂ composites. This observation highlights the fact that the organic dyes (MG and MB) act as a good photosensitizer by increasing the photocatalytic activity of nano TiO₂ for the photodegradation of PS under UV radiation. It was also noticed that the decrease in band intensities were higher for PS-TiO₂-MB composites compared to that of PS-TiO₂-MG composites. The increase in degradation efficiency of PS-(TiO₂-5%MB), PS-(TiO₂-5%MG) with respect to pristine PS were 5.13 and 5.25 respectively.

6.4.4. Mechanical properties

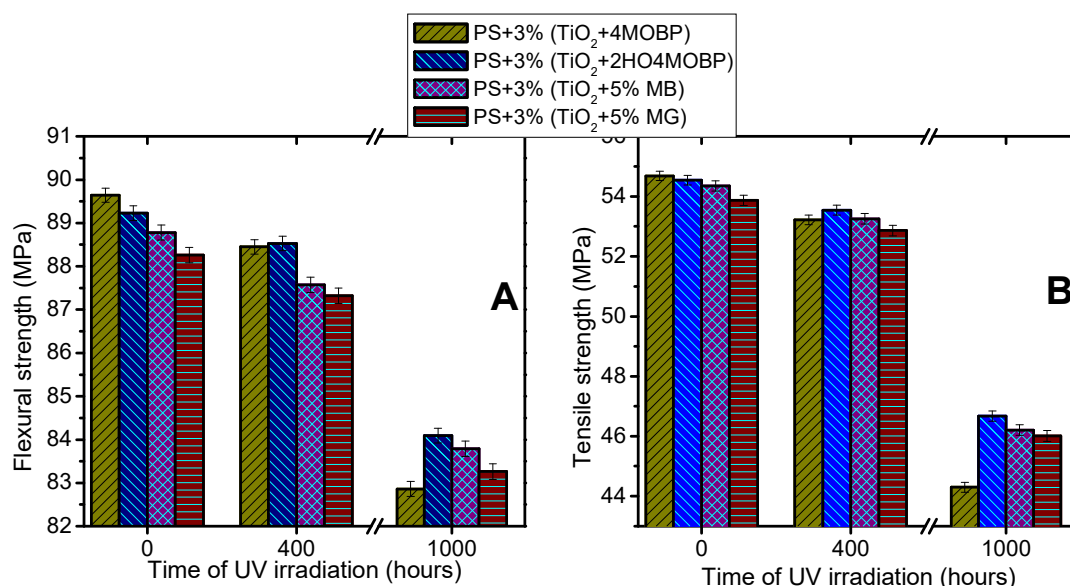


Figure 6.12. Flexural (A) and tensile (B) strengths of PS-TiO₂-benzophenone based photosensitizer and PS-TiO₂-organic dye composites exposed to UV radiation for 0, 400 and 1000 h

The mechanical properties of PS+3%(TiO₂+4MOBP) which exhibited maximum photodegradation and PS+3%(TiO₂+2H4MOBP) which exhibited minimum photodegradation among the PS-TiO₂-benzophenone based photosensitizer composites were studied after UV irradiation of 0, 400 and 1000 hours (Figure 6.12). The mechanical properties of PS+3%(TiO₂ + 5%MB) and PS+3%(TiO₂+ 5%MG) upon UV irradiation were also studied. The tensile and flexural strengths of all the composites decreased as the time of UV irradiation increased. PS+3% (TiO₂+4MOBP) exhibited better degradation compared to PS+3%(TiO₂+2H4MOBP) as expected among the PS-TiO₂-benzophenone based photosensitizer composites.

Even though PS+3%(TiO₂+5%MB) underwent better photodegradation compared to PS+3%(TiO₂+5%MG), the decrease in mechanical properties were significant in PS+3%(TiO₂+5%MG). This anomaly might have arisen as a consequence of poor dispersion of MG compared to that of MB in the PS-TiO₂-dye composites.

6.4.5. Electrical properties

The BDV of PS-3%(TiO₂+4MOBP), PS-3%(TiO₂+2ClBP) and PS-3%(TiO₂+5%MB) composites at varying UV irradiation time intervals (0, 400 & 1000 hours) were measured (Figure 6.13.1). All these composites underwent an appreciable decrease in the value of BDV as the time of UV irradiation increased. The decrease in BDV observed in PS-3%(TiO₂+2ClBP) was slightly greater than that of PS-3%(TiO₂+4MOBP) after UV irradiation.

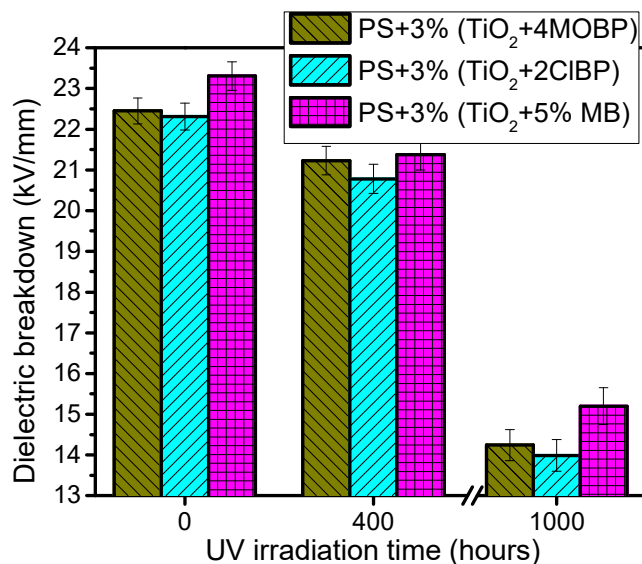


Figure 6.13.1. Dielectric breakdown (breakdown voltage) of PS-TiO₂-4MOBP, PS-TiO₂-2ClBP and PS-TiO₂-MB composites at varying UV irradiation time

Dielectric permittivity (ϵ_r) of PS-3%(TiO₂+4MOBP), PS-3%(TiO₂+2ClBP) (Figure 6.13.2), PS-3%(TiO₂+5% MB) and PS-3%(TiO₂+5% MG) (Figure 6.13.3) were measured at UV irradiation intervals of 0, 400 and 1000 hours. The ϵ_r of all the composites under study increased upon UV irradiation time. It is observed from the figure 6.13.2 that PS-3%(TiO₂+2ClBP) underwent better increase in the values of ϵ_r on UV irradiation compared to PS-3%(TiO₂+4MOBP). Similarly PS-3%(TiO₂+5% MB) showed better increase in ϵ_r compared to PS-3%(TiO₂+5% MG) upon UV irradiation (Figure 6.13.3).

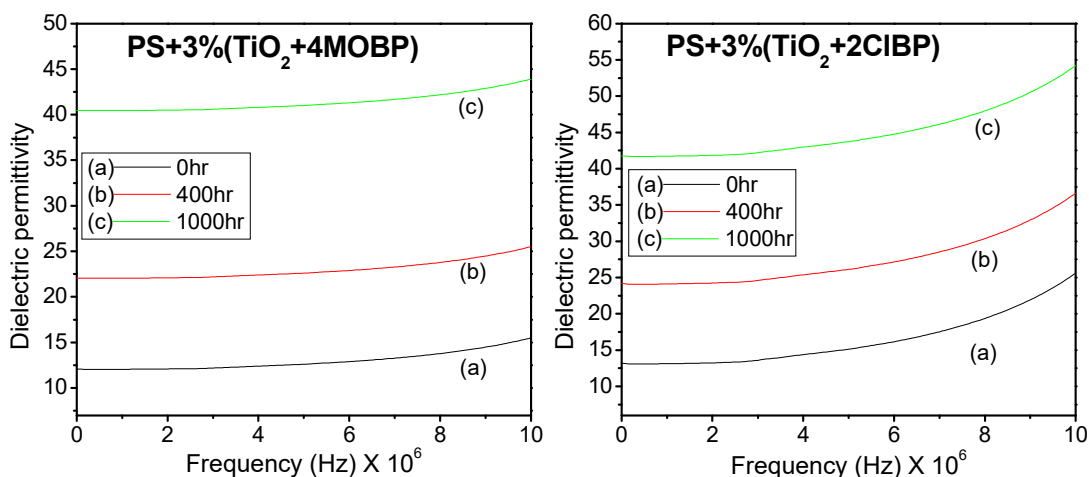


Figure 6.13.2. Dielectric permittivity of PS-3% 4MOBP and PS-3% 2ClBP composites at UV irradiation intervals of 0, 400 and 1000 h

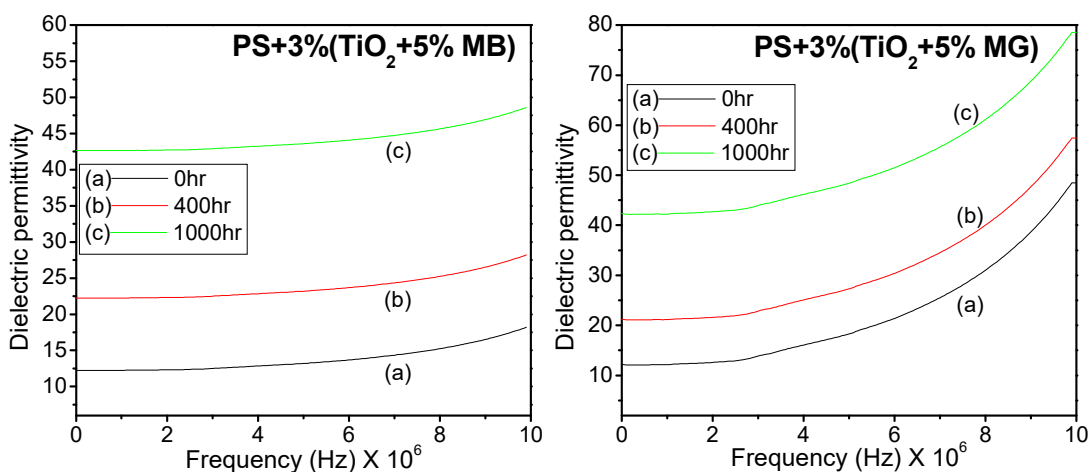


Figure 6.13.3. Dielectric permittivity of PS-3% MB and PS-3% MG composites at UV irradiation intervals of 0, 400 and 1000 h

6.4.6. Thermogravimetric Analysis (TGA)

The thermogram of PS-3%(TiO₂+4MOBP) (Figure 6.14 A) and PS-3% (TiO₂+5%MB) (Figure 6.14 B) obtained from TGA of the composites in nitrogen atmosphere gave two stages of weight loss curves representing the water desorption and decomposition of the composites respectively. Shift in decomposition temperature were observed in the composites upon UV irradiation. The decomposition temperature range of PS-3%(TiO₂+4MOBP) shifted from 293-423°C to 273-410°C on UV irradiation of 1000 hours. Similarly, a shift in decomposition temperature range for PS-3%(TiO₂+5%MB) was observed from 300-433°C to 287-424°C on UV irradiation of 1000 hours. Beyond the termination point of steep decomposition curve

of PS-3%(TiO₂+4MOBP) at 423°C (wt %=10) and PS-3%(TiO₂+5%MB) at 433°C (wt %=12.13), a slow decrease in weight percentage was observed. This represents the presence of inorganic residues that were quite thermally stable at these temperatures. UV irradiation of 1000 hours resulted to the decrease in the termination point of steep decomposition curves of the composites to lower temperature.

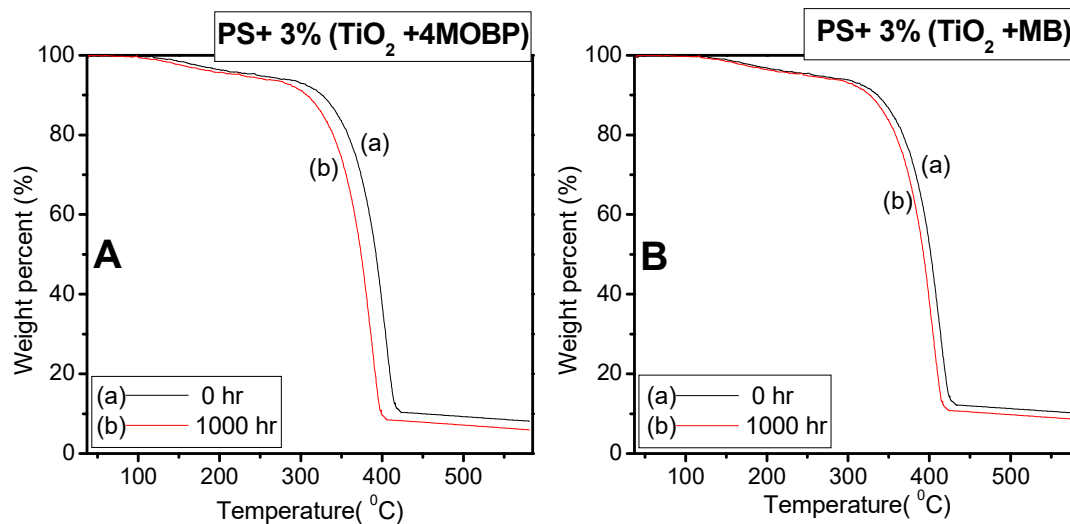


Figure 6.14. TGA thermogram of PS-3% (TiO₂+4MOBP) (A) and PS-3% (TiO₂+5%MB) (B) composites before and after UV irradiation of 1000 h

6.4.7. Weight loss

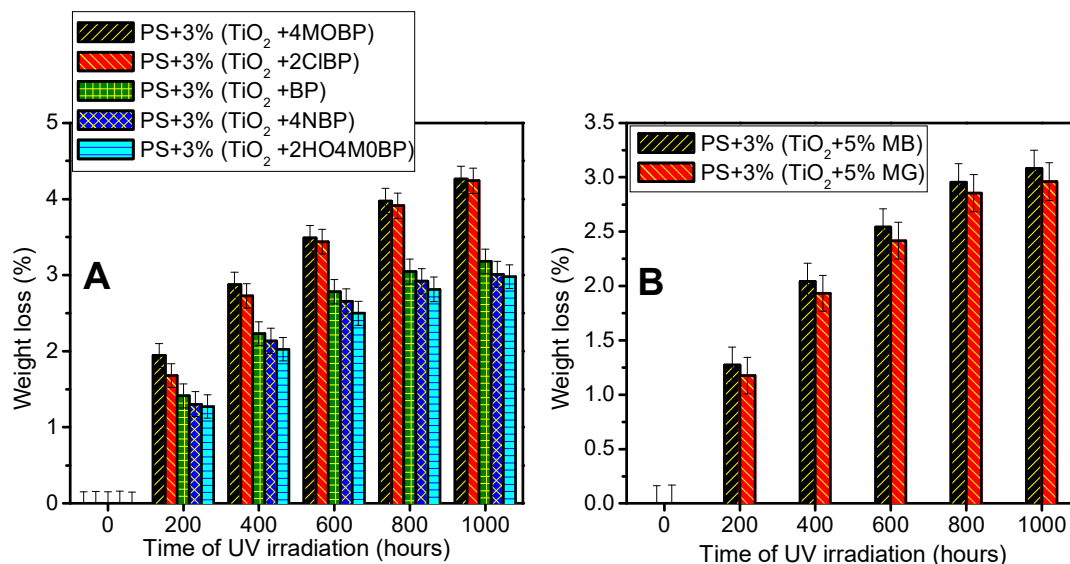


Figure 6.15. Comparison of weight loss percentages of PS-3% (TiO₂+benzophenone based photosensitizer) (A) and PS-3% (TiO₂+dye) (B) composites at regular intervals of UV irradiation

Significant weight loss was observed for PS-(TiO₂+benzophenone based photosensitizer) (Figure 6.15 A) and PS-(TiO₂+dye photosensitizer) (Figure 6.15 B) composites at regular intervals of UV irradiation. The order of weight loss percentage was PS-3%(TiO₂+4MOBP) > PS-3%(TiO₂+2ClBP) > PS-3%(TiO₂+BP) > PS-3%(TiO₂+4NBP) > PS-3%(TiO₂+2HO4MOBP). The weight loss percentage of PS-organic dye was found to be in the following order:- PS-3%(TiO₂+MB)> PS-3%(TiO₂+MG).

6.4.8. Scanning Electron Microscopy (SEM)

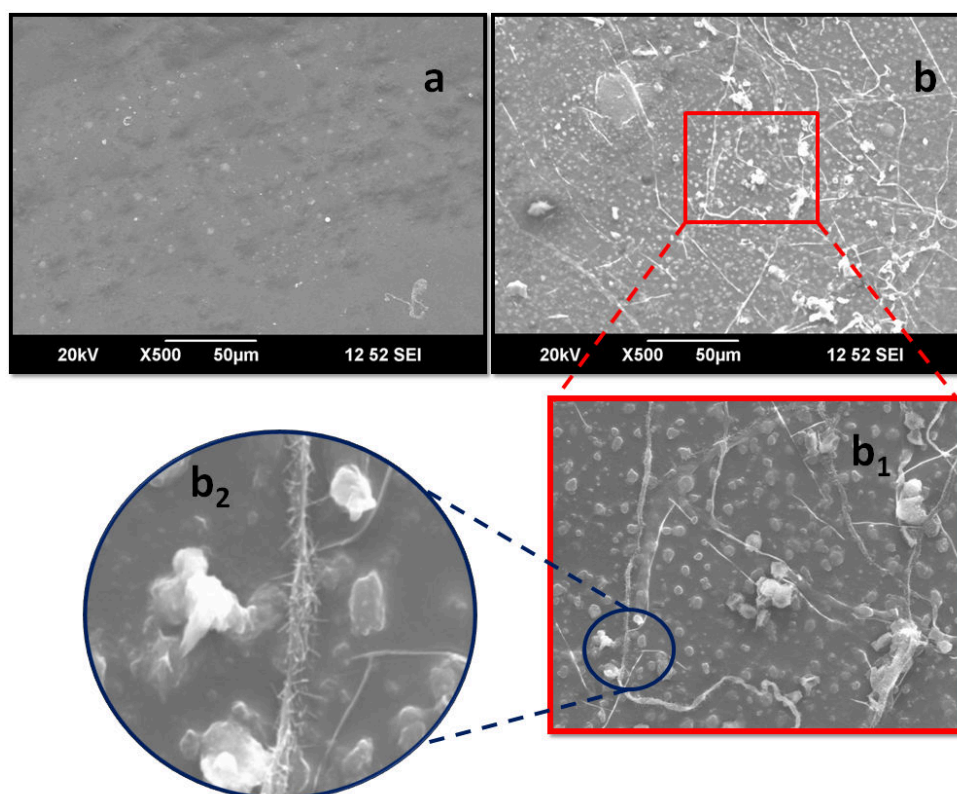


Figure 6.16. SEM image of PS-3%(TiO₂+4MOBP) composite before (a) and after (b) UV irradiation of 1000 hours. 'b₁' and 'b₂' represents a portion of image 'b' in high resolution

The SEM image of PS-3%(TiO₂+4MOBP) showed an increase in surface roughness after 1000 hours of UV exposure. Figure 6.16 a represents the polymer composite sheet before UV irradiation. After UV irradiation of 1000 hours (Figure 6.16 b) the polymer surface seemed to have increased roughness due to deterioration. Focused images of UV exposed sample (Figure 6.16 b₁ and b₂) revealed the

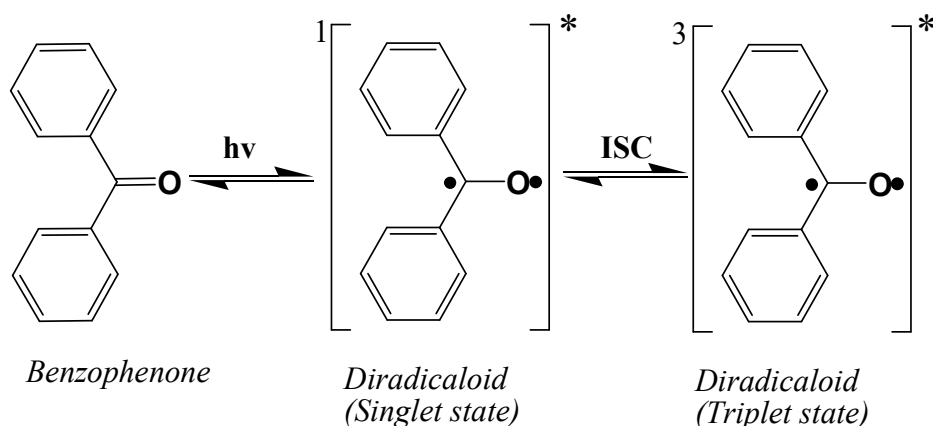
possibility that the surface of the polymer sheet might have degraded thereby exposing the catalysts over the surface.

6.5. Mechanism of photosensitized PS degradation

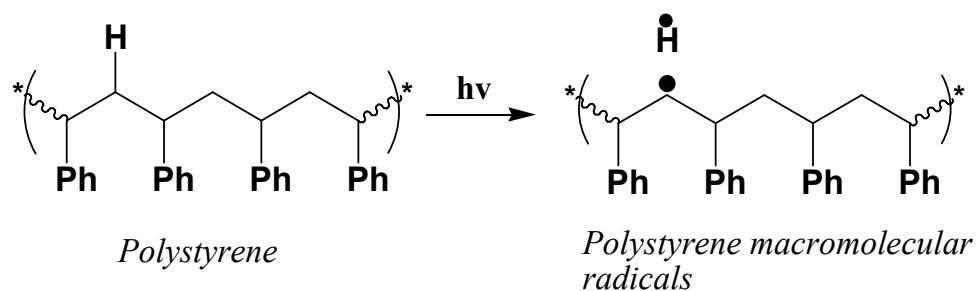
Based on the observations and discussions done so far, we could conclude that benzophenone derivatives act as a photosensitizer for the effective degradation of PS, harvesting UV radiation. The degradation efficiency of PS loaded with these compounds were however not as effective as nano TiO₂. When nano TiO₂ was coupled with benzophenone derivatives, their efficiency for the degradation of PS under UV light increased upto an appreciable level. The dyes, MB and MG on the other hand, had no appreciable photosensitizing efficiency by themselves, for PS degradation. They however acted as good photosensitizer when coupled with nano TiO₂. Both the benzophenone derivatives and organic dyes, MB and MG enhanced the photocatalytic activity of TiO₂.

An important observation made from the FTIR spectra of PS-benzophenone derivatives was the increased double bond formation upon UV irradiation. The possible mechanism for this is as depicted below.

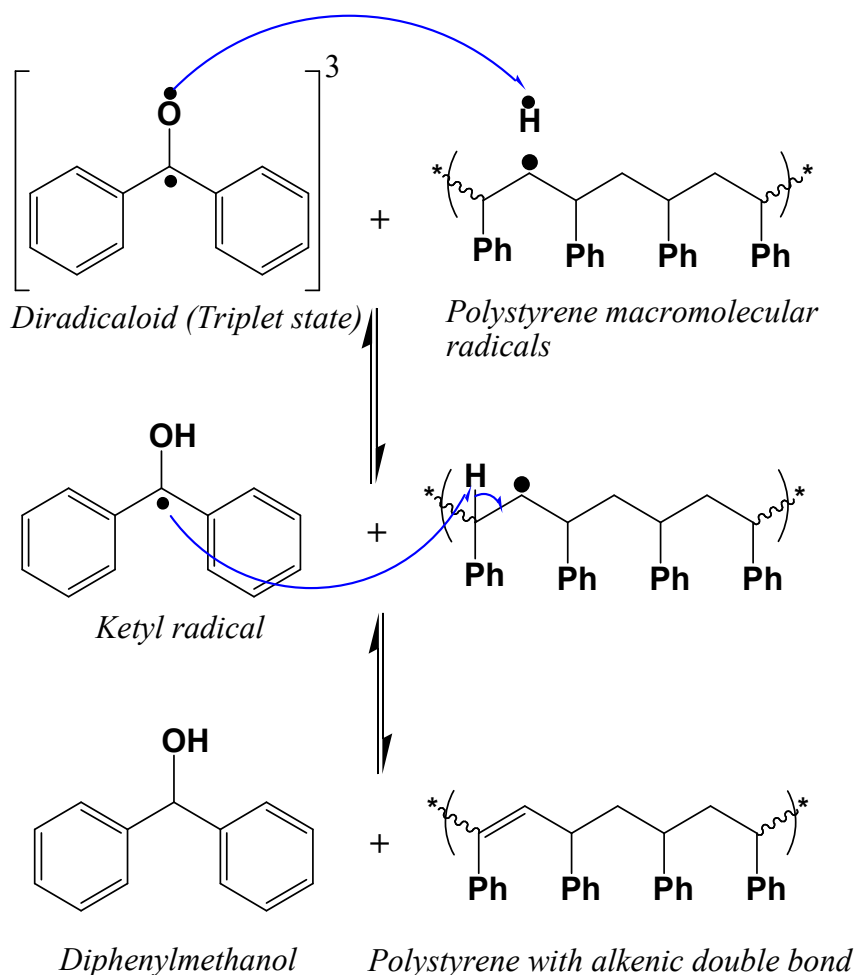
- The π -bond belonging to the $>C=O$ group in benzophenone may undergo homolytic cleavage in the presence of UV radiation to form singlet state diradicaloid. The diradicaloid is converted from singlet state to triplet state through inter system crossing (ISC) as given below.



- The sigma bonds between C-C and/or C-H of PS may also undergo homolytic cleavage in the presence of UV radiation as given below to form macromolecular radicals.



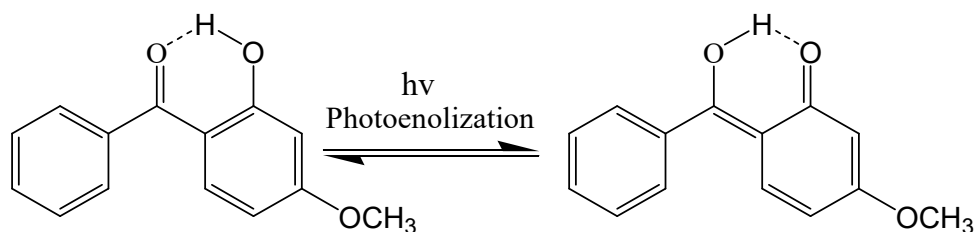
- Interaction between diradicaloid of benzophenone and PS radical takes place. The benzophenone diradicaloid abstracts hydrogen radical ($\text{H}\cdot$) generated from PS to form ketyl radical. The ketyl radical can further abstract another $\text{H}\cdot$ from the adjacent carbon resulting in the formation of alkenic carbon-carbon double bond in the PS chain (as evident from FTIR of UV irradiated PS).



It should also be noted that the polystyrene macromolecular radicals may also react with oxygen or water from the atmosphere leading to $-\text{OH}$, $-\text{OOH}$ as well as $>\text{C}=\text{O}$ radicals in the PS chain (as evident from FTIR). The mechanism has been described in detail in chapter 3.

The above proposed mechanism depends mainly upon two aspects. Primarily the diradicaloid formed out of benzophenone should be stable without recombination and secondly the presence of PS macromolecular radicals should be in the vicinity of benzophenone diradicaloid for effective interaction. SEM image clearly revealed uniform dispersion of the composites where interaction among the PS and catalysts are possible. The diradicaloid are stable upto an extent as they are in conjugation with the two adjacent phenyl rings.

Observations made from the results of various analyses proved that the presence of various substituted groups on the phenyl rings of benzophenone influenced its photosensitizing activity. Loading PS with 4MOBP and 2CIBP resulted in a slight increase in the rate of photodegradation compared to BP, 4NBP and 2HO4MOBP. The exact reason for this observation has to be studied in detail. The decrease in the photocatalytic activity of 2HO4MOBP, however could be explained on the basis of photoenolization due to intra molecular hydrogen bond formation as depicted below.



2-hydroxy-4-methoxybenzophenone

2HO4MOBP undergoes tautomerisation in the presence of UV light termed as photoenolization. The hydrogen bond existing between $-OH$ and $>C=O$ groups present in 2HO4MOBP also favours photoenolization. Due to the co-existence of hybrid structures as depicted in the above diagram of 2HO4MOBP as a result of photoenolization, the chance for the formation of diradicaloid is almost hindered. This results in the inefficiency of 2HO4MOBP to act as a photosensitizer for the photodegradation of PS^{27,28}.

6.6. Conclusion

Photodegradation of PS in the presence of benzophenone derivatives and triphenylmethane dyes as photosensitizers was studied. The combination of these dyes with nano TiO_2 for the photodegradation of TiO_2 was also investigated. All the PS-

benzophenone based photosensitizer composites showed accelerated degradation compared to pristine PS under UV irradiation. However the extent of degradation was not up to PS-TiO₂. Among the PS-benzophenone based photosensitizer composites, photodegradation followed the order: PS-4MOBP, PS-2CIBP, PS-BP, PS-NBP, PS-2H4MOBP. The decrease in the efficiency of 2H4MOBP for the photodegradation of PS could be explained due to photoenolization. The extent of photodegradation of PS-dye composites were not much appreciable. The combination of benzophenone based photosensitizer and dyes with nano TiO₂ showed an appreciable increase in the photodegradation efficiency even compared to PS-TiO₂ composites. Highest photocatalytic efficiency for the degradation of PS among TiO₂-benzophenone based photosensitizer composites was exhibited by TiO₂-4MOBP followed by TiO₂-2CIBP composite. PS-(TiO₂-MB) exhibited better photodegradation compared to PS-(TiO₂-MG) among the PS-TiO₂-dye composites. It can be concluded that the combination of benzophenone based photosensitizers or triphenylmethane dyes with TiO₂ serves as an efficient photocatalyst for the degradation of PS under UV irradiation.

References

1. Manangan, T., Shawaphun, S. & Wacharawichanant, S. Acetophenone and Benzophenone Derivatives as Catalysts in Photodegradation of PE and PP Films. in *Functionalized and Sensing Materials* **93**, 284–287 (Trans Tech Publications Ltd, 2010).
2. Barboiu, V. & Avadanei, M. I. Chemical reactions of benzophenone photoirradiated in 1,2-polybutadiene. *J. Photochem. Photobiol. A Chem.* **222**, 170–179 (2011).
3. Geuskens, G., Delaunois, G., Lu-Vinh, Q., Piret, W. & David, C. Photo-oxidation of polymers—VIII. The photo-oxidation of polystyrene containing aromatic ketones. *Eur. Polym. J.* **18**, 387–392 (1982).
4. Torikai, A., Takeuchi, T. & Fueki, K. Photodegradation of polystyrene and polystyrene containing benzophenone. *Polym. Photochem.* **3**, 307–320 (1983).
5. Lin, C. S., Liu, W. L., Chiu, Y. S. & Ho, S.-Y. Benzophenone-sensitized photodegradation of polystyrene films under atmospheric conditions. *Polym. Degrad. Stab.* **38**, 125–130 (1992).
6. Pinto, L. F. A., Goi, B. E., Schmitt, C. C. & Neumann, M. G. Photodegradation of polystyrene films containing UV-visible sensitizers. *J. Res. Updat. Polym. Sci.* **2**, 39–47 (2013).
7. Sikkema, K., Cross, G. S., Hanner, M. J. & Priddy, D. B. Photo-degradable polystyrene Part I: enhancing the photo-degradability of polystyrene by the addition of photosensitizers. *Polym. Degrad. Stab.* **38**, 113–118 (1992).
8. Cuquerella, M. C., Lhiaubet-Vallet, V., Cadet, J. & Miranda, M. A. Benzophenone Photosensitized DNA Damage. *Acc. Chem. Res.* **45**, 1558–1570 (2012).
9. Bayrakçeken, F. Triplet–triplet optical energy transfer from benzophenone to naphthalene in the vapor phase. *Spectrochim. Acta Part A Mol. Biomol. Spectrosc.* **71**, 603–608 (2008).
10. Bergamini, G. *et al.* Forward (singlet–singlet) and backward (triplet–triplet) energy transfer in a dendrimer with peripheral naphthalene units and a benzophenone core. *Photochem. Photobiol. Sci.* **3**, 898–905 (2004).
11. Si, Y., Liang, W. & Zhao, Y. Theoretical Prediction of Triplet–Triplet Energy Transfer

- Rates in a Benzophenone–Fluorene–Naphthalene System. *J. Phys. Chem. C* **116**, 12499–12507 (2012).
12. Foote, C. S. DEFINITION OF TYPE I and TYPE II PHOTOSENSITIZED OXIDATION. *Photochem. Photobiol.* **54**, 659 (1991).
 13. Aumaitre, C. *et al.* Visible and near-infrared organic photosensitizers comprising isoindigo derivatives as chromophores: synthesis, optoelectronic properties and factors limiting their efficiency in dye solar cells. *J. Mater. Chem. A* **6**, 10074–10084 (2018).
 14. Nagarajan, B. *et al.* Novel ethynyl-pyrene substituted phenothiazine based metal free organic dyes in DSSC with 12% conversion efficiency. *J. Mater. Chem. A* **5**, 10289–10300 (2017).
 15. Swanson, S. A. *et al.* Stable and Efficient Fluorescent Red and Green Dyes for External and Internal Conversion of Blue OLED Emission. *Chem. Mater.* **15**, 2305–2312 (2003).
 16. Leung, M. *et al.* 6-N,N-Diphenylaminobenzofuran-Derived Pyran Containing Fluorescent Dyes: A New Class of High-Brightness Red-Light-Emitting Dopants for OLED. *Org. Lett.* **8**, 2623–2626 (2006).
 17. Stolarski, R. & Fiksinski, K. J. Fluorescent perylene dyes for liquid crystal displays. *Dye. Pigment.* **24**, 295–303 (1994).
 18. Grabchev, I., Moneva, I., Bojinov, V. & Guitonneau, S. Synthesis and properties of fluorescent 1,8-naphthalimide dyes for application in liquid crystal displays. *J. Mater. Chem.* **10**, 1291–1296 (2000).
 19. Mitra, S. A polymeric triarylmethane dye as a sensitizer for photoconductivity. *J. Polym. Sci. Polym. Symp.* **74**, 165–169 (1986).
 20. Tanielian, C., Mechin, R. & Shakirullah, M. Origin of dye bleaching and polymer degradation in the methylene blue-sensitized photo-oxygenation of polybutadiene. *J. Photochem. Photobiol. A Chem.* **64**, 191–199 (1992).
 21. Chakrabarti, S., Chaudhuri, B., Bhattacharjee, S., Das, P. & Dutta, B. K. Degradation mechanism and kinetic model for photocatalytic oxidation of PVC–ZnO composite film in presence of a sensitizing dye and UV radiation. *J. Hazard. Mater.* **154**, 230–236 (2008).
 22. Duxbury, D. F. The photochemistry and photophysics of triphenylmethane dyes in solid and liquid media. *Chem. Rev.* **93**, 381–433 (1993).
 23. Baptista, M. & Indig, G. Effect of BSA Binding on Photophysical and Photochemical Properties of Triarylmethane Dyes. *J. Phys. Chem. B - J PHYS CHEM B* **102**, (1998).
 24. Fleischmann, C., Lievenbrück, M. & Ritter, H. Polymers and dyes: developments and applications. *Polymers (Basel)*. **7**, 717–746 (2015).
 25. Nguyen, T. K. N. *et al.* Titanium dioxide-benzophenone hybrid as an effective catalyst for enhanced photochemical degradation of low density polyethylene. *e-Polymers* **18**, (2018).
 26. Mishra, A., Fischer, M. K. R. & Bäuerle, P. Metal-Free Organic Dyes for Dye-Sensitized Solar Cells: From Structure: Property Relationships to Design Rules. *Angew. Chemie Int. Ed.* **48**, 2474–2499 (2009).
 27. Placzek, M., Dendorfer, M., Przybilla, B., Gilbertz, K.-P. & Eberlein, B. Photosensitizing properties of compounds related to benzophenone. *Acta Derm. Venereol.* **93**, 30–32 (2013).
 28. Allen, N. S., Luc-Gardette, J. & Lemaire, J. Photostabilising action of ortho-hydroxy benzophenones in polypropylene film: Influence of processing and wavelength of irradiation. *Polym. Photochem.* **3**, 251–265 (1983).